THESIS
2

MICHIGAN STATE UNIVERSITY LIBRARIES
3 1293 01712 9101

This is to certify that the

thesis entitled

"An Infiltrometer To Measure And
Analyze The In-situ Sorptivity."

presented by

Fei-Jan Kao

has been accepted towards fulfillment
of the requirements for

M.S. degree in Agricultural Engineering

Major professor

Date March 23, 1998

O-7639

MSU is an Affirmative Action/Equal Opportunity Institution

LIBRARY
Michigan State
University

PLACE IN RETURN BOX
to remove this checkout from your record.
TO AVOID FINES return on or before date due.

DATE DUE	DATE DUE	DATE DUE

1/98 c:/CIRC/DateDue.p65-p.14

AN INFILTROMETER TO MEASURE AND ANALYZE THE IN-SITU SORPTIVITY

By

Fei-Jan Kao

A THESIS

Submitted to
Michigan State University
in partial fulfillment of the requirements
for the degree of

MASTER OF SCIENCE

Department of Agricultural Engineering

1998

ABSTRACT

AN INFILTROMETER TO MEASURE AND ANALYZE THE IN-SITU SORPTIVITY

By

Fei-Jan Kao

The proposed infiltrometer is an non-electronic system to measure the soil sorptivity in the field. It is low-cost, portable, reliable, and simple for installation and use. In additional to the soil sorptivity, this infiltrometer can also be used to determine the soil hydraulic conductivity and macroscopic capillary length. In our research, we suggest a new method instead of the conventional cumulative infiltration vs. time$^{1/2}$ diagram to analyze the field data. Even when the true infiltration is not measured at the very start, we can still obtain the correct sorptivity using the suggested analysis. Two new parameters, initial infiltration and lag time, are introduced in the sorptivity determination. In order to calculate the soil sorptivity more accurately, it is necessary to evaluate the initial infiltration in the field. The lag time is the duration between the onset of the soil infiltration and the start of the measurement and should be used to examine the reliability of the result of field experiments.

ACKNOWLEDEGMENTS

I would like to express my sincere gratitude to my committee chairman, Dr. George Merva, for his advice, help, and encouragement given during the course of my studies and research.

I am also grateful for the help and guidance offered by the other members of my committee, Dr. Robert Von Bernuth and Dr. Harold Belcher.

I would also like to thank Richard Wolthuis for his help and advice.

Finally, a special thank to my parents and my girl friend, Ya-Hsien Chen, for supporting me through each of the deadlines for the completion of this thesis which came and went.

TABLE OF CONTENTS

List of Tables vi

List of Figures vii

I. Introduction 1

II. Literature Review 5

  A. Non-tension Infiltrometer 5

  B. Tension Infiltrometer 7

  C. Problems with Current In-Situ Infiltrometer 11

III. Fundamentals 13

IV. Objectives 15

V. System Design 16

  A. Proposed System 16

  B. System Prototype 18

VI. Instructions for Field Use 23

  A. Setting the Potential 23

  B. Site Preparation 23

  C. System Installation 23

  D. Soil Sample Water Content 24

  E. Required Measurement Time 25

VII. Test System I 26

  A. Test 1 Results 26

  B. System Modifications 29

- C. Test 2 Results 32
- D. Problems and Analysis 32
- E. Re-analysis of Test 2 42

VIII. Error Analysis 45
- A. Empirical Equation for Real Flow 45
- B. Experiment Design 46
- C. Regressions and Results 46
- D. Discussions 49

IX. Test System II 50
- A. Results for Site 1 50
- B. Results for Site 2 53
- C. Results for Site 3 57
- D. Discussions 61

X. Recommendations 67

XI. Conclusions 73

Appendices

- A. Component Specifications 75
- B. Experimental Data for Field Tests 77
- C. Experimental Data for Error Analysis 87

List of References 88

LIST OF TABLES

Table 1. Experimental data for Test 1. 27

Table 2. Comparison of regression results generated by different numbers of points. 44

Table 3. Comparison of results from different tests at site 1. 53

Table 4. Comparison of results from different tests at site 2. 57

Table 5. Comparison of results from different tests at site 3. 57

Table 6. Comparison of results from different tests at site 3. 61

Table 7. The recommended range of lag time for different soils. 71

LIST OF FIGURES

Figure 1. Proposed system for sorptivity measurement. 17

Figure 2. Designed sample cup. 19

Figure 3. Prototype for sorptivity measurement. 20

Figure 4. Designed flow meter. 22

Figure 5. Cumulative infiltration vs. time$^{1/2}$ diagram for Test 1. 28

Figure 6. Modified system for sorptivity measurement. 30

Figure 7. Relative position of the soil surface and top of the sample cup. 31

Figure 8. Cumulative infiltration vs. time diagram for Test 2. 33

Figure 9. Cumulative infiltration vs. time$^{1/2}$ diagram for Test 2. 34

Figure 10. Cumulative infiltration vs. time diagram for constant head and falling head flow. 35

Figure 11. Cumulative infiltration vs. time diagram for ideal sorptivity flow and experimental sorptivity flow. 37

Figure 12. Cumulative infiltration vs. time$^{1/2}$ diagram for ideal sorptivity flow and experimental sorptivity flow. 38

Figure 13. Cumulative infiltration v. time diagram for ideal sorptivity flow and experimental sorptivity flow with initial infiltration. 40

Figure 14. Square of cumulative infiltration vs. time diagram for ideal sorptivity flow and experimental sorptivity with initial infiltration. 41

Figure 15. Cumulative infiltration^2 vs. time diagram for Test 2. 43

Figure 16. Designed system for error analysis. 47

Figure 17. Regression curve for the result of error analysis. 48

Figure 18. Result of the first for Capac loam. 51

Figure 19. Result of the second test for Capac loam. 52

Figure 20. Result of the first test for Riddles-Hillsdale sandy loam. 54

Figure 21. Result of the second test for Riddles-Hillsdale sandy loam. 55

Figure 22. Result of the third test for Riddles-Hillsdale sandy loam. 56

Figure 23. Result of the first test for Granby loamy fine sand. 58

Figure 24. Result of the second test for Granby loamy fine sand. 59

Figure 25. Result of the third test for Granby loamy fine sand. 60

Figure 26. Result of steady state flow for the first test at site 3. 62

Figure 27. Result of steady state flow for the second test at site 3. 63

Figure 28. Result of steady state flow for the third test at site 3. 64

Figure 29. Recommended sample cup and porous plate. 69

Figure 30. Recommended water reservoir with adding tube. 70

Figure 31. Recommended flow meter with parallel tubing. 72

I. Introduction

Today, the demand for the high quality water is increasing while depletion of the fresh water supply is occurring all over the world. Agricultural practices are a major cause of this depletion and, in some areas, cause considerable degradation of the water quality as well as the supply. This problem can be improved by effective management of agricultural water use and a good understanding of soil and water interaction.

Engineers are particularly interested in the soil infiltration and movement of water through the soil profile. This understanding is necessary for hydrological modeling and irrigation planning, since infiltration is the sole source of soil water to support the growth of vegetation and of the ground water supply of wells, springs, and streams. In addition, construction of roads, dams, and buildings also require detailed knowledge of soil properties, including soil infiltration. Many researchers have been studying soil infiltration for decades.

Philip (1969) intensively studied the infiltration of ponded water into soil and proposed that infiltration depends on two major parameters, sorptivity and hydraulic conductivity. Sorptivity is a soil water property that innately contains information on the soil hydraulic conductivity and diffusivity. Generally, sorptivities can be measured more accurately and easily than unsaturated hydraulic conductivity and diffusivity, so it is worthwhile to consider determining the latter parameters in this indirect way.

In order to measure the sorptivity in the field on undisturbed soil, there is an obvious need for a simple and reliable device. To serve this need, several instruments have been designed and built in the past for to be used in practical field applications.

In 1969, Talsma (1969) designed the very first infiltrometer to measure the in-situ sorptivity by applying Philip's equation. Similar to Talsma's device, a twin ring method (Scotter et al.,1982) involved measuring the steady state infiltration of ponded water. In addition, the Guelph permeameter (Reynolds and Elrick, 1985), and a portable, microcomputer-controlled drip infiltrometer designed by Bridge and Ross(1985) were also used in the field. However, Taslsma's device and the other devices for the determination of the in-situ sorptivity are restricted to water supply potential greater than zero. They have the disadvantages that supply potential decreases during measurement and the macropores of soil possibly influence the result of the sorptivity measurement (Perroux and White, 1988).

To prevent macropores from dominating saturated sorptivity measurements, Dixon (1975) designed the single-ring, single-square and double-square closed-top infiltrometers to measure saturated sorptivity under a small suction. Similar to Dixon's device, Dirksen (1975) designed an apparatus for determination of sorptivity by one dimensional absorption into short columns of a loamy sand. Nowadays, Perroux and White's technique (1988) is widely used in many designs of instruments to determine the in-situ sorptivity. An automated tension infiltrometer designed by Arkeny et al. (1988), and another tension infiltrometer built by Logsdon and Jaynes (1993) were a modification of an early version of Perroux and White's disk permeameter. However, the disk permeameter is not able to restrict the infiltration to one direction and can not ensure good contact between soil surface and porous disk. Moreover, the method suggested by Talsma (1969) to determine the field sorptivity using a tension infiltrometer creates some errors in the data analysis during the determination of sorptivity.

The system proposed in this work is an infiltrometer to measure the soil sorptivity under a supplied water potential (-10 mm to -150 mm) in the field. It is low-cost, portable, reliable, but simple to install and use. The infiltrometer uses a sharpened edge metal cylinder for the sample cup to avoid soil disturbance and air infiltration into the soil during conduct of the test; furthermore, the cup ensures flow in one direction during early infiltration. A designed flow meter is used to determine the infiltration rate during operation of measurement. In additional to the soil sorptivity, this instrument can be used to rapidly determine other hydraulic properties (e.g. hydraulic conductivity, macroscopic capillary length, etc.) of field soil. A modification of Talsma's method to analyze the soil sorptivity from the field data is proposed in this paper. In addition, two new parameters, initial infiltration and lag time, are introduced for the determination of the in-situ sorptivity. The initial infiltration and lag time are recommended to be criteria for examining the reliability of the result for each experiment.

II. Literature Review

A. Non-tension Infiltrometer

Talsma (1969) described a typical method for determining sorptivity in the field. The measurements were made on large samples enclosed within 300 mm diameter, 150 mm high, infiltrometer rings pushed into the soil. Water was rapidly ponded in the rings to depth of about 30 mm; the subsequent drop in water level was noted at regular time intervals from 10 to 15 seconds, on a sharply inclined aluminum scale graduated at 2 mm intervals over 200 mm length. The scale was suspended from the rim of the infiltrometer with adjustable bolts, allowing variation of the angle of inclination to the horizontal soil surface, which varied in practice from 4° to 15° (giving an accuracy of depth measurement between 0.07 and 0.25 mm), depending on the rate of drop of water level. Talsma's device is restricted to water supply potentials greater than zero. It has the disadvantage that water supply potential decreases during measurement (Perroux and White, 1988).

Similar to Talsma's device, a twin ring method which was mentioned by Scotter et al. (1982) involved measuring the steady state infiltration of ponded water from two rings of different radii that had been lightly pressed 10 mm into the soil, just far enough to prevent lateral leakage when water was ponded. The radii of rings range from 0.025 to 0.204 m depending on the soil types which were tested. This method of measuring sorptivity is simple and needs a minimum of equipment. This method also tried to minimize soil disturbance and error in measurement due to smearing, compaction or cracking. The twin ring method is also limited to positive supply potential and has the disadvantage that supply potential decreases during measurement.

Reynolds and Eleric (1985) applied the Guelph permeameter to determine the in situ sorptivity. In the field, two wells with radii 0.02 m and 0.03 m, were used. The wells were dug with different diameters of augers. The depth of the wells varied from 0.25 to 0.35 m below the soil surface. Within each well, an initial depth of ponding of 0.1 m was used to obtain first flow rate corresponding to the initial depth, and followed immediately afterward with a second depth of 0.15 m to obtain second flow rate corresponding to the second depth. The sorptivity and hydraulic conductivity can then be computed. Reynolds and Elrick tried to minimize the influence of smearing and compaction of well wall by the auger, siltation of the well during the course of measurement, and entrapment of air during the initial filling of the well. Like Talsma's device, the Guelph permeameter can only measure the sorptivity and hydraulic conductivity with supply potential greater than zero and has the same disadvantage of supply potential decreasing during measurement.

A portable, microcomputer-controlled drip infiltrometer, designed by Bridge and Ross (1985), was used to determine the sorptivity and hydraulic conductivity in the field. The main components of the drip infiltrometer are gravity supply tank, a measuring cylinder with water level sensor and solenoid inlet and outlet valves, a 1 m^2 dripper unit and swing support, a stepper motor to swing the dripper, and a microcomputer control system. The microcomputer controls the amount of water delivered from and added to the measuring cylinder. When more water must be delivered to satisfy the set rate, the microcomputer opens the outlet valve, switches on the stepper motor and moves the unit through 100 mm to the other side of its travel. The outlet valve is then closed, the stepper motor switched off and the cylinder refilled if necessary. The dripper unit is constructed of lightweight PVC conduit and is fixed on the swing frame. The measuring cylinder, level sensor, solenoid valves and stepper are assembled as an integrated unit mounted on a support stand. The advantage of the drip infiltrometer is that it is an automatically recording device. The disadvantages are i) the whole unit is comparatively large and can not easily change sites, ii) high building and maintenance costs, and iii) operation only at water supply potential greater than zero.

B. Tension Infiltrometer

Dixon (1975) designed the single-ring, single-square and double-square closed-top infiltrometer. The first of three closed-top infiltrometers designed and used was the single-ring device. This infiltrometer consists of an acrylic ring (150 mm I.D.) closed at the top except for connections to two water manometers and to an air pressure regulator. To initiate an infiltration run, the closed-top ring is (i) closed at the bottom with a disk of plastic film, (ii) filled with water , (iii) placed upon the soil surface area to be tested, (iv) opened at the bottom by slipping out the film, and (v) sealed on the soil surface with a wet soil paste. Cumulative infiltration can be determine by observing manually the drop of water level in the closed-top ring. For automatic recording, the water manometer air lines are connected to the two bellows of an air pressure recorder. Automatic recording by this method is limited to some specific modes of operation. The single-ring infiltrometer was designed to simulate effective surface heads ranging from -30 mm to +10 mm of water. This device appears somewhat cumbersome, and is only for routine field use (Perroux and White, 1988).

Dirksen (1975) designed an apparatus for determination of sorptivity by one dimensional absorption into short columns of a loamy sand. In the field, the soil is contained in a sharp-edged cylinder (10 mm long and 150 mm in diameter) which is pushed into the soil and the soil surface cut even with the top of the cylinder. Contact can be improved at times by sieving a very thin layer of local, dry soil over the cylinder before placing the ceramic plate on the top of it. The plate diameter should be kept as large as possible to smooth the effect of soil inhomogeneities and to facilitate accurate volumetric measurements. Water is supplied to the soil surface through a porous ceramic plate from a horizontal graduated pipette. The receding water meniscus in the pipette (4 mm I.D.) could be read to 0.001 ml^3. The pressure head was maintained constant by means of a Mariotte-type regulator before the plate was placed against the soil surface. This allowed for accurate determination of initial volume and starting time. Air could escape at the bottom of the soil columns. Dirksen's permeameter provides a simple concept of design; however it is not used much in the field.

Clothier and White (1981) simplified Dirksen's device and designed a sorptivity tube for field measurements. The sorptivity tube is basically a Mariotte bottle in which supply potential was determined by the bubbling pressure of a capillary or hypodermic needle through which air entered a water reservoir. In the field, the soil is contained in a thin walled perspex cylinder (95 mm long and 86 mm I.D.) which is pushed into the soil and the soil surface cut even with the top of the cylinder. Water was supplied to the soil via a sintered glass plate sealed at the upper end by a stopcock. Once the stopcock is closed, water can move into the cylinder through the porous plate only if air enters through the hypodermic needle. The practical range of supply potential was from -0.1 m to 0 m water. The sorptivity tube has been used in a variety of hydrological and soil management studies; however, for soil with high sorptivity, the air entry through the hypodermic needle was insufficient to maintain supply potential constant. This is the major limitation of this device (Perroux and White, 1988).

Perroux and White (1988) modified the sorptivity tube for application as a disk permeameter. In their design, the hypodermic needle in the sorptivity tube is replaced by a bubbling tower. The water level in the bubbling tower is used to control the supply potential. The cylinder in the sorptivity tube is replaced by a 200 mm diameter disk to reduce the soil disturbance. The disk is made of clear material to enable the operator to check for air leakage. The bottom of the disk is milled to form a shallow reservoir, which is enclosed by a water supply membrane, a fine mesh nylon screen. The membrane is supported by a steel mesh backing and two or more layers of material. The infiltrometer is constructed of polycarbonate plastic. Both the water reservoir tubes and bubbling tower have metal distance scales attached. The reservoir and bubbling tower can be detached from permeameter during transportation. This also permits the use of reservoirs of various diameters which depends on the type of soil which is tested. The disk permeameter can be operated at both supply potential less than zero and greater than zero.

Arkeny et al. (1988) designed an automated tension infiltrometer whose major components are a bubble tower, a Mariotte column (water reservoir), a base for soil contact, and a transducer-equipped data logger for data collection and storage. The bubble tower has four air-entry ports that control tension by allowing air entry at different distances below the water level. The port can be present to tensions from 0.02 m to 0.5 m, and valves are used to switch from one port to another. The bubble tower is connected to the water reservoir with 1.6 mm I.D. polypropylene tubing (bubbling tube). Interchangable water reservoir of different diameters are employed because the volume of water infiltrating into the soil is calculated from the height change of water in the reservoir. A mesh nylon filter is used for soil contact. The filter is backed by a circular acrylic faceplate which has approximately one 2 mm hole per 10 mm^2 to allow water flow. Measurement of infiltration can be automated by the use of data logger and two pressure transducers and the operation range of the automated tension infiltrometer is from 0.02 to 0.5 m of water tension and for infiltration rates of 1 x 10^{-8} to 5 x 10^{-4} m/s.

Logsdon and Jaynes (1993) designed a tension infiltrometer which was a modification of an early version of Perroux and White's disk permeameter. Variations from the disk permeameter were that reservoir and bubble tube were not interchangable, membranes were used in place of interfacing for the spacing material in the base, and the infiltrometers were automated with transducers, as described by Ankeny et al. (1988). The wetting area diameter of the infiltrometer base was 230 mm. Soil was scraped off level before making the measurements since most of the measurements were made subsurface; therefore, no contact material was necessary to obtain hydraulic contact between infiltrometer and soil.

C. Problems with Current In-Situ Infiltrometer

Presently, the disk permeameter is most commonly used to determine the in-situ sorptivity. However, there are some problems encountered when applying the disk permeameter in the field. The sorptivity is derived from one dimensional flow (Philip, 1969); nevertheless, the disk permeameter is not able to restrict the infiltration in one direction. This means the derived sorptivity may contain error and may not represent the true characteristic of the field soil. In addition, the disk permeameter does not ensure good contact between soil surface and porous disk. This allows air leaking into the soil sample during the experiment and influencing the outcome of the field test. Another disadvantage of the disk permeameter is the limitation of measurement. For the disk permeameter, the infiltration rate is determined by recording the differential of falling water levels in the reservoir. Because of the limitation of minimizing the cross sectional area of the water reservoir, for slow infiltration (e.g. clay), it will take a long time to obtain enough data to generate the soil sorptivity.

All of the previously mentioned devices allow some early infiltration into soil before the beginning of the measurement because it is difficult to design an non-electrical infiltrometer to set up the supply tension to the desired value immediately at the start of the infiltration. However, people overlooked the early infiltration and omitted it. This will create significant errors in the result of the sorptivity measurement.

III. Fundamentals

Talsma (1969) applied Philip's (1969) infiltration theory and presented the following equation to model the early stage of one dimensional water infiltration into the soil.

$$i = \frac{I}{\pi r_0^2} \approx S_0 t^{\frac{1}{2}} \qquad (1)$$

Where:

i = cumulative infiltration

I = cumulative volume of infiltration

r_0 = radius of soil sample

t = time from start of infiltration

S_0 = sorptivity

In Eq. (1), the sorptivity S_0 is the slope of the plot of i vs. $t^{½}$.

White and Sully (1987) introduced the macroscopic capillary length λ_c defined by

$$\lambda_c = \frac{bS_0^2}{(\theta_{wet} - \theta_{dry})K_0} \qquad (2)$$

Where:

θ_{dry} = the initial volumetric water content

θ_{wet} = the final water content at the supply potential Ψ_0

K_0 = unsaturated hydraulic conductivity at Ψ_0

b = 0.55, a representative value for soil

Wooding (1968) used a disk under steady state conditions and obtained

$$\frac{Q_0}{\pi r_0^2} \approx K_0 + K_0 \frac{4\lambda_c}{\pi r_0} \qquad \textbf{(3)}$$

Where:

Q_0 = steady state flow rate of infiltration

The first term on the right of Eq. (3) essentially represents the contribution of gravity to the total flow and the second term contains the contribution due to capillarity.

The relationship between the hydraulic conductivity K_0 and the sorptivity S_0 is obtained by combining Eq.s (2) and (3).

$$K_0 = \frac{Q_0}{\pi r_0^2} - \frac{4bS_0^2}{\pi r_0(\theta_{wet} - \theta_{dry})} \qquad \textbf{(4)}$$

Thus, to estimate the unsaturated hydraulic conductivity from Eq. (4), one must determine the Sorptivity, the steady flow rate, the initial volumetric water content, and the final water content at the supply potential Ψ_0.

IV. Objectives

The objectives of this project are as follows:

i. To develop an infiltrometer that is portable, durable, reliable, and simple in design with an accuracy of ± 10% of readings.

ii. To design a system that prevents air infiltration into the soil during the test, and that has a water capacity for long term operation.

iii. To test the system in sand, silt, loam and clay texture soils.

iv. To analyze the field data and consider the propriety of the conventional method of the sorptivity determination.

V. System Design

The sorptivity infiltrometer system is intended to be portable, durable, reliable, but simple in design and has an accuracy of ± 10%. The instrument prototype should be able to execute a test without air infiltration into the soil during conduct of the test, and should have a water capacity for long term operation. In addition, the system should be satisfactory for sand, silt, loam, or clay textured soils.

A. Proposed System

The system (Fig. 1) as designed in prototype is comprised of four components: sample cup, water reservoir, potential tube, and flow meter.

A sample cup was chosen because it will restrict flow in the soil to one dimension, and will prevent air leakage into the sample during execution of the test. The sample cup is made of steel and designed to be driven into the soil.

The water reservoir supplies water for in-situ tests and holds enough water for a long term experiment. The potential tube is of clear plastic so that the height of the water column can be viewed, making it

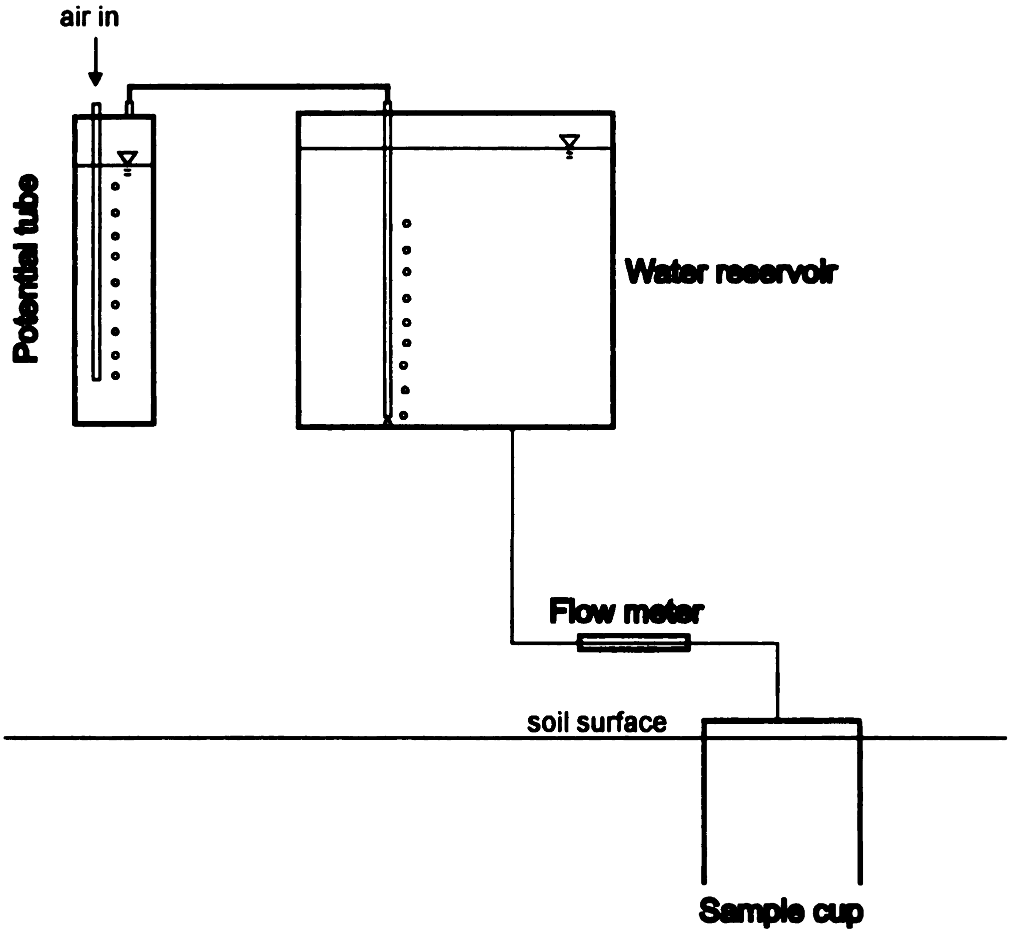
air in
Potential tube
Water reservoir
Flow meter
soil surface
Sample cup

Figure 1. Proposed system for sorptivity measurement.

possible to control the potential during the test. The water reservoir and the potential tube are connected by tygon tubing.

A flow meter consisting of a length of clear tubing of relatively small diameter resting next to a calibrated surface is used to determine the rate of flow of water during the test. In operation, a bubble of air is injected into the tubing, and the time required for the bubble to travel a set distance is used to determine the rate of flow. If the roughness of the tubing is very small, the velocity of the bubble should be close to the velocity of water in the flow meter

B. System Prototype

The sample cup (Fig. 2) consists of a cylinder 104 mm diameter and 125 mm long, with a removable top fastened together by four screws. The removable top has the advantage that the condition of the soil surface within the core can be observed. If necessary, a layer of porous sand can be applied to the soil surface prior the test. The removable top contains an inlet and an outlet (to expel the trapped air). A gasket is used to seal the top to the sample chamber.

The water supply reservoir (Fig. 3) is constructed of a clear polycarbonate tube, 200 mm inside diameter and 200 mm long with a capacity of 6 liters. The top of the reservoir contains a water inlet, an air outlet and a water outlet connecting to the potential control tube. The air outlet will accept a small pump which can be used to exhaust air from the reservoir prior to commencing the infiltration, if desired.

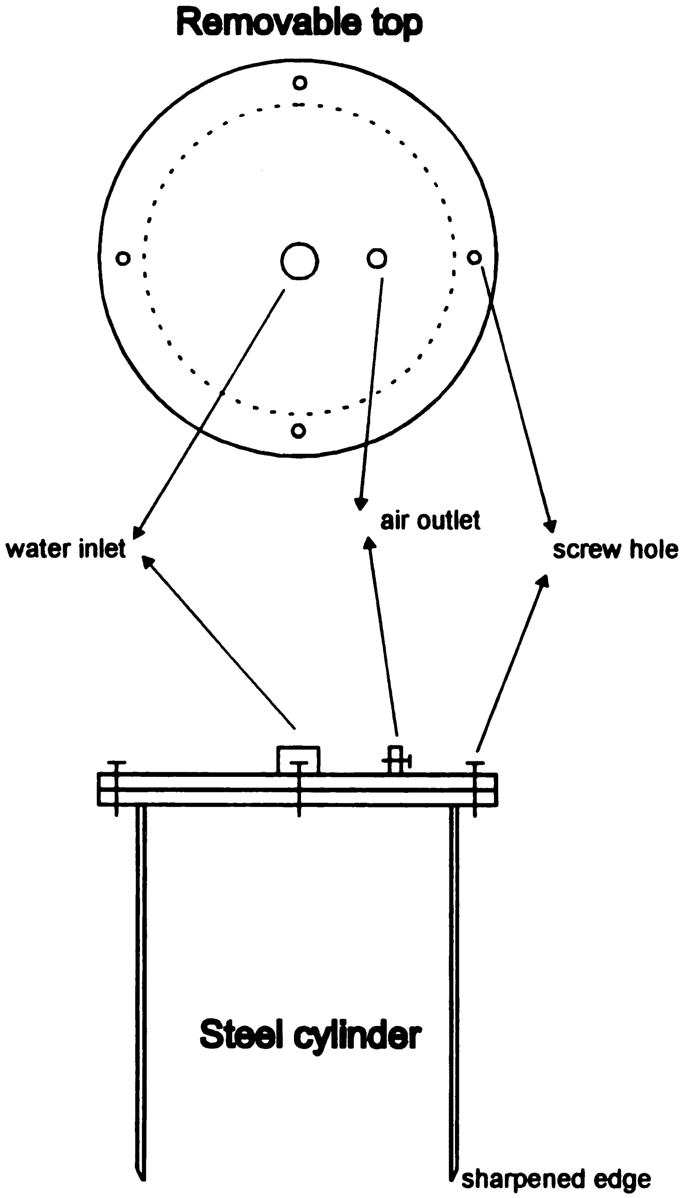
Removable top
water inlet
air outlet
screw hole
Steel cylinder
sharpened edge

Figure 2. Designed sample cup.

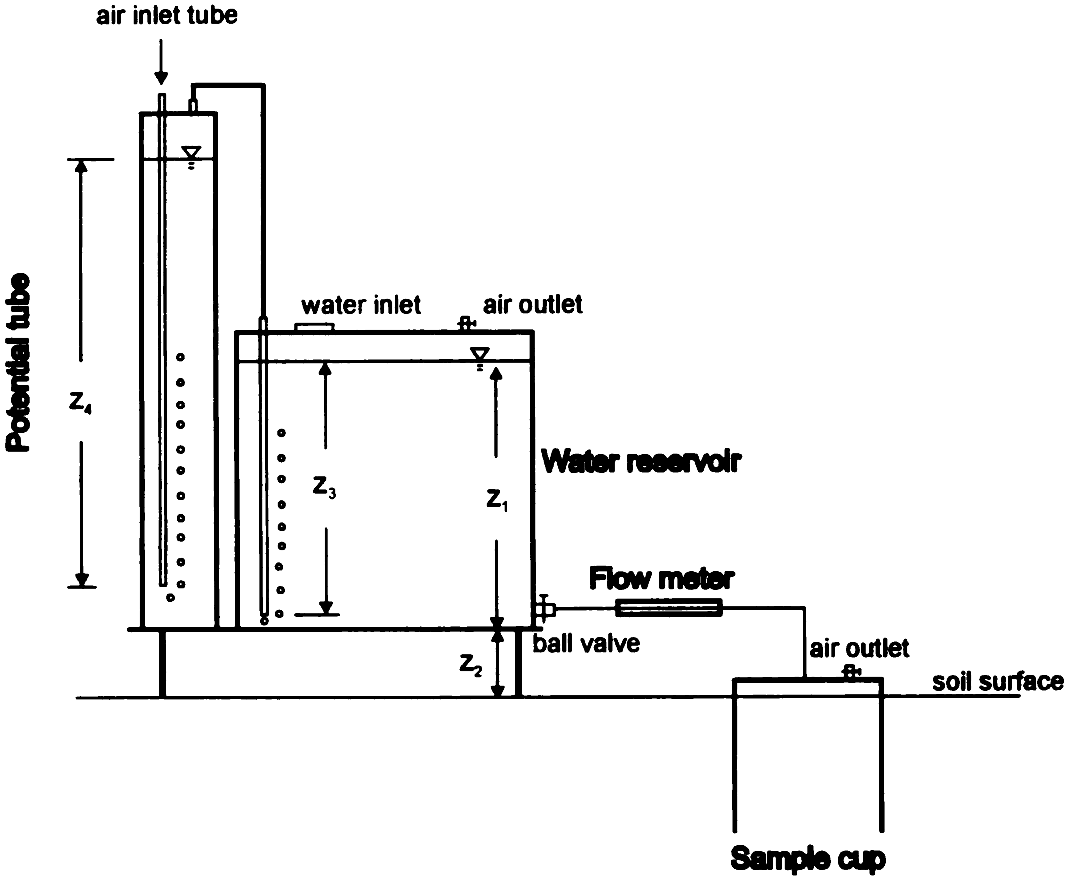
air inlet tube
Potential tube
Z_4
water inlet
air outlet
Z_3
Z_1
Water reservoir
Flow meter
ball valve
Z_2
air outlet
soil surface
Sample cup

Figure 3. Prototype for sorptivity measurement.

The potential tube is 50 mm inside diameter and 350 mm long. It contains an air inlet tube of 3 mm inside diameter which can be adjusted vertically throughout it entire length thus determining the potential at which water may enter the soil in the sample cup. The supply potential can be set from -10 mm to -150 mm water height. Both the reservoir and the potential tube rest on a small wooden stand.

The flow meter (Fig. 4) connects the water reservoir and the sample cup. A segment of 3.2 mm inside diameter tubing lies adjacent to a ruler. Air is injected into the flow meter using a hypodermic syringe. At the far end of the flow meter, a vertical tube traps the bubble, preventing it from entering the soil. The designated distance of bubble movement is L_b and the duration of bubble movement is t_b. Thus the volumetric rate of the water within the meter is determined by L_b/t_b multiplying the cross sectional area of the tubing in flow meter.

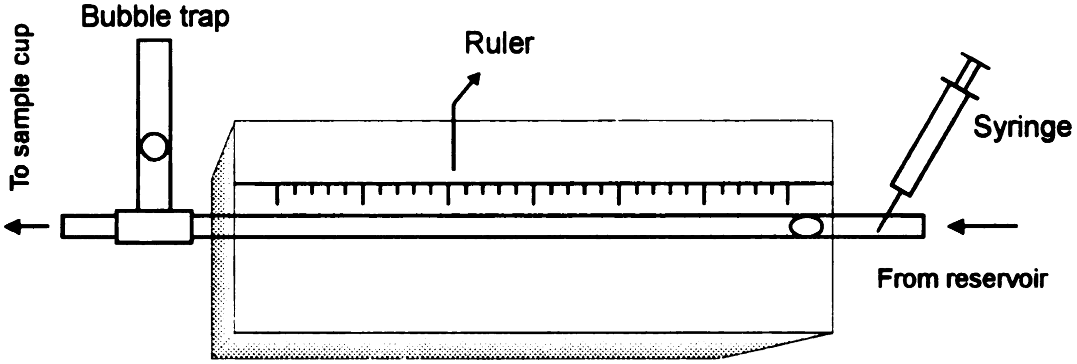
To sample cup
Bubble trap
Ruler
Syringe
From reservoir

Figure 4. Designed flow meter.

VI. Instructions for Field Use

A. Setting the Potential

Before testing the system in the field, supply potential is set by altering the height of the air inlet tube in the potential control tube as shown in Fig. 3. The supply potential at the soil surface is $z_1 + z_2 - z_3 - z_4$. The value of z_2 is the height of the wooden stand and is fixed. Since the value of z_1 decreases while the infiltration proceeds and z_3 has the same decreasing rate as z_1, $z_1 + z_2 - z_3$ will remain constant. The supply potential is varied by only changing z_4, the height of the air inlet tube.

B. Site Preparation

The instrument is only tested on bare soil. If the soil is not flat and even, it will be necessary to level it.

C. System Installation

In the first period, testing was performed in sandy soil only since sandy soil responds quickly. The system was tested on the Michigan State University research farm using following procedures:

i) Hammer the cylinder 100 mm deep into the soil, and level the soil sample (if necessary) with a spatula, trying not to disturb the condition of the top soil. Attach the top of sample cup using the four screws.

ii) Place the water reservoir beside the sample cup, connect it to the flow meter and the potential tube with the interconnecting tubing.

iii) Set the depth of the air inlet tube, z_4, to the desired position.

iv) Make sure the air outlet of the sample cup is open, and then fill the sample cup with water by turning on the ball valve. Once water exits from the air outlet, shut off air outlet at both the water reservoir and sample cup immediately.

v) When the air inlet tube begins bubbling, start measuring as soon as possible. Inject 0.1 ml air into the flow meter every minute and record the time of bubble movement t_b through the designated distance L_b by using a portable computer.

D. Soil Sample Water Content

The initial water content, supply water content, and the bulk density are needed to calculate the hydraulic conductivity. At least two samples should be taken for each test to determine the initial water content and bulk density. Samples are taken approximately 250 mm from the center of the sample cup.

After the completion of infiltration, dig out the sample cup with a shovel, remove the tubing, and quickly reverse the sample cup to allow excessive water to drain out. Sample the top 2 to 3 mm of soil for supply water content determination.

Once the samples are taken, they should be placed in tin cans and capped with a lid , then stored in plastic bags and sealed for transportation.

E. Required Measurement Time

Both the duration of sorptivity and time of approaching to steady state depend on the soil. The duration of sorptivity flow can rage from 0.02 to 1 hour. The time required to approach steady state flow ranges from 0.2 to 6 hours (Perroux and White, 1988).

VII. Test System I

A. Test 1 Results

The flow rate, Q, at every minute is derived from multiplying the velocity of the bubble, L_b/t_b, by the cross sectional area of the tubing in the flow meter. Moreover, the cumulative infiltration, i, at any time t is the total amount of water, I, which has flowed into the soil divided by the cross sectional area of the sample cup, A_0. The calibrated cross sectional area of flow meter and sample cup is 7.92 mm^2 and 8413 mm^2. According to Eq. (1), the sorptivity S_0 calculated from the early time data near the origin of the i vs. $t^{1/2}$ diagram. The slope of the straight line portion is S_0, the sorptivity, and it has the dimensions of length / $time^{1/2}$.

Test 1 was run on Oct. 5th, 1997. The results are shown in Table 1 and the i vs. $t^{1/2}$ diagram is shown as Fig 5. The curve relating i to $t^{1/2}$ for water in Fig.5 is found to be non-linear, making the determination of a sorptivity impossible. Theoretically, the relationship between the cumulative infiltration and $time^{1/2}$ during the early infiltration, i and $t^{1/2}$ should behave close to a straight line. This unexpected result is due to the fact that the readings from which the i to $t^{1/2}$ ratio was found right after the air inlet tubing began bubbling. However, some infiltration occurred before the bubbling began.

Table.1. Experimental data of Test 1

Test 1
Date: 10/5/97
Location: Research farm land at M.S.U.
Soil type: Granby loamy fine sand
Supply potential: -20 mm
L_b = 150 mm

Time (min)	**t_b (sec)**	**Q (ml)**	**$Time^{1/2}$ ($sec^{1/2}$)**	**I (ml)**	**i (mm)**
0	0.00	0.00	0.00	0.00	0.00
1	7.57	9.12	7.75	9.12	1.08
2	7.87	8.77	10.95	17.89	2.13
3	8.07	8.55	13.42	26.44	3.14
4	8.27	8.35	15.49	34.79	4.13
5	8.47	8.15	17.32	42.94	5.10
6	8.63	8.00	18.97	50.94	6.05
7	8.63	8.00	20.49	58.94	7.00
8	8.70	7.93	21.91	66.87	7.94
9	8.91	7.75	23.24	74.62	8.87
10	8.96	7.70	24.49	82.32	9.78
11	8.97	7.70	25.69	90.02	10.69
12	9.09	7.59	26.83	97.61	11.60
13	9.10	7.59	27.93	105.19	12.50
14	9.16	7.54	28.98	112.73	13.39
15	9.20	7.51	30.00	120.24	14.28
16	9.20	7.51	30.98	127.74	15.18
17	9.23	7.48	31.94	135.22	16.07
18	9.39	7.35	32.86	142.57	16.94
19	9.55	7.23	33.76	149.80	17.80
20	10.02	6.89	34.64	156.69	18.62
22	9.77	14.14	36.33	170.82	20.29
24	9.82	14.07	37.95	184.89	21.97
26	9.89	13.97	39.50	198.85	23.62
28	9.62	14.35	40.99	213.20	25.33
30	9.62	14.35	42.43	227.54	27.03
32	9.69	14.255	43.82	241.80	28.73

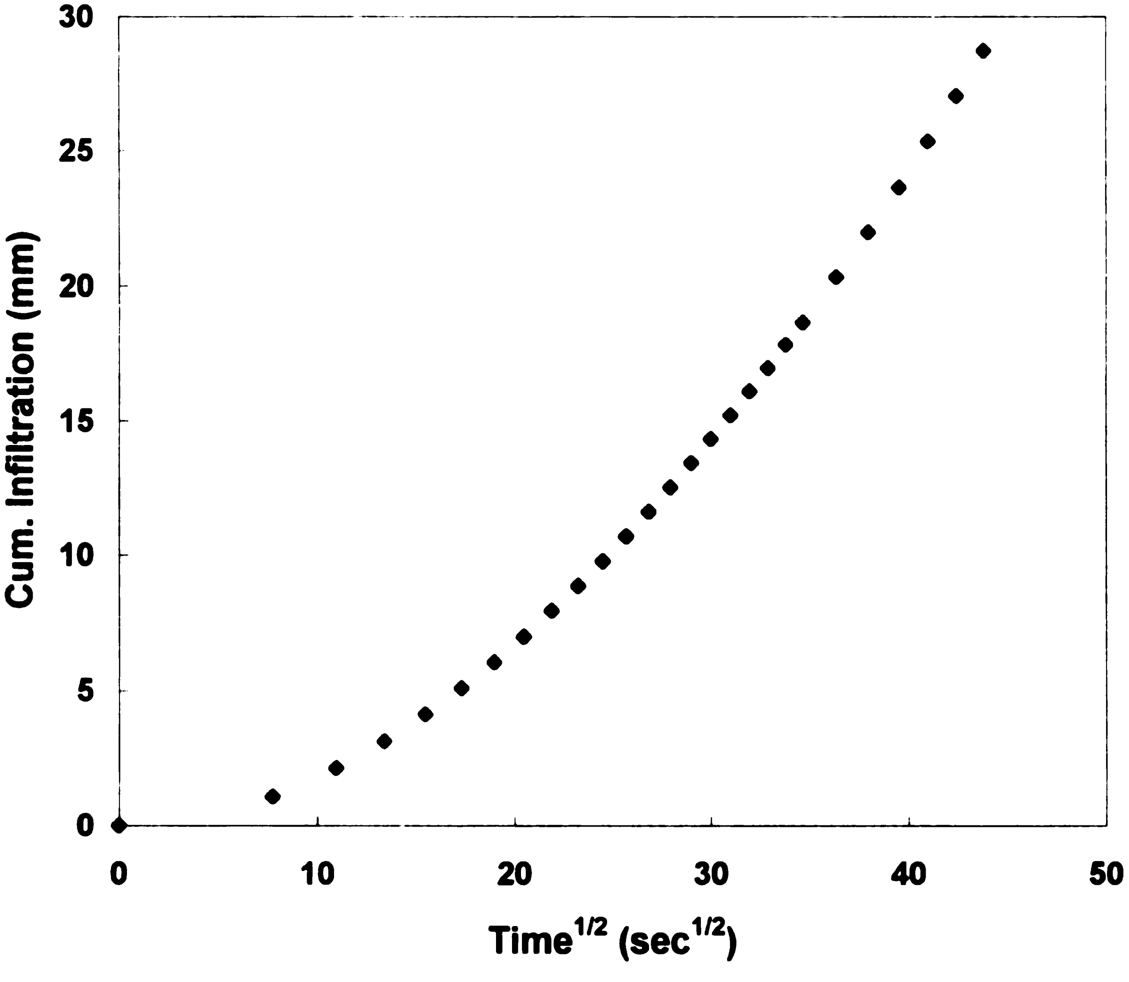

Figure 5. Cumulative infiltration vs. time$^{1/2}$ diagram for Test 1.

Therefore, the start point of the cumulative infiltration in Fig. 5 was not at the origin. In order to get the actual results of the field test, it is necessary to estimate the amount of infiltration which has taken place before the bubbling starts.

B. System Modifications

In order to evaluate the volume of the initial infiltration I_0 ,infiltration which occurs before bubbling begins, a portable digital scale was placed under the water reservoir as Fig 6. The z_2 distance now will be the height of the scale. The capacity of the scale chosen was 30 kg and the readability is 0.001kg. The scale was not sensitive enough to estimate the sorptivity flow but it is enough to evaluate the initial infiltration. When the specific weight of water is unity as 1, the volume of gross initial infiltration I_{gross}, the amount of total filling water before the time of bubbling happens, can be decided by the digital scale.

Another quantity, V_0, must be determined in order to evaluate I_0. In Fig 7, V_0 is the volume between the soil surface and the inlet of the removable top and it varies according to the height of h_0. In most tests, h_0 is forced to be 10 mm by filling a thin layer of dry fine sand or placing a porous plate on the soil surface. Thus, I_0 can be calculated by

$$I_0 = I_{gross} - V_0 \qquad (5)$$

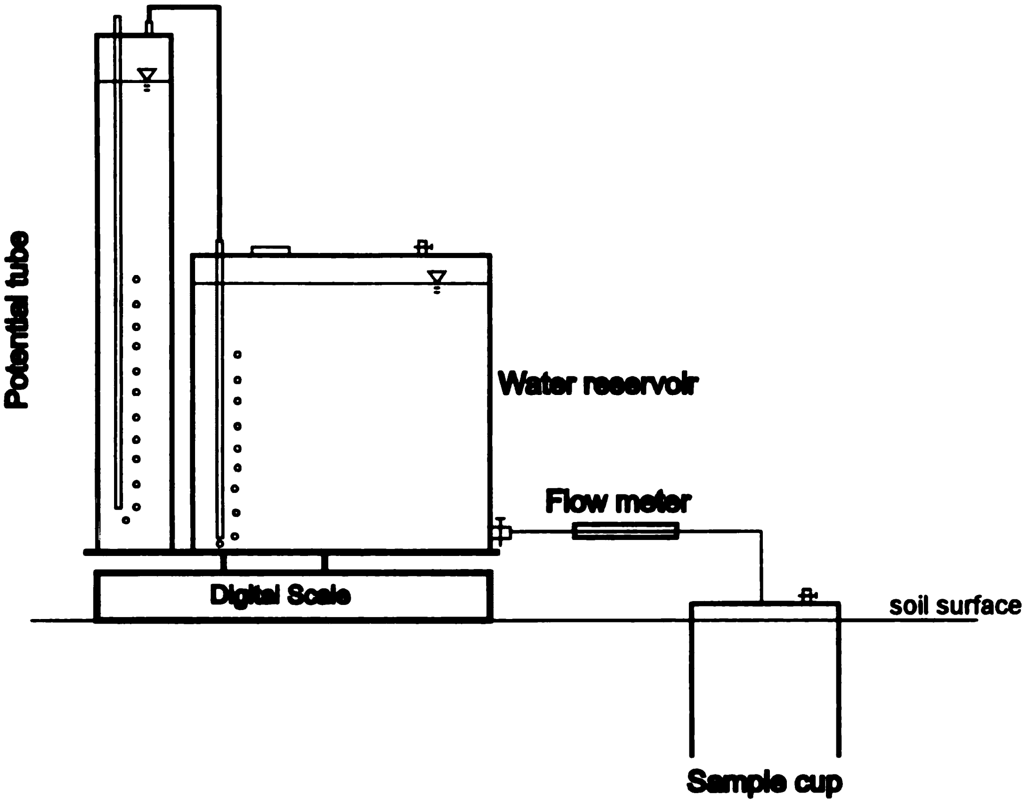
Potential tube
Water reservoir
Flow meter
Digital Scale
soil surface
Sample cup

Figure 6. Modified system for sorptivity measurement.

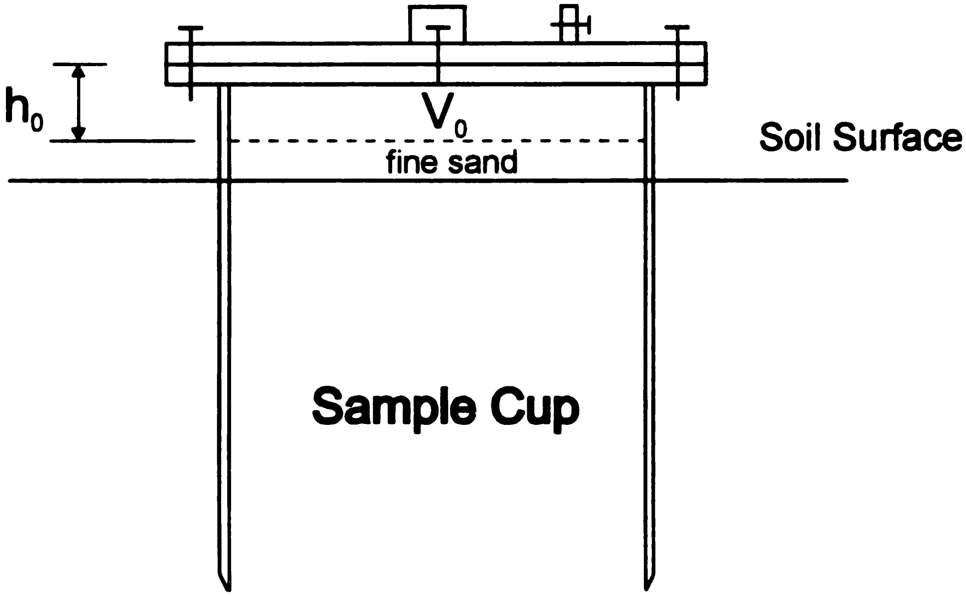
h_0
V_0
fine sand
Soil Surface
Sample Cup

Figure 7. Relative position of the soil surface and top of sample cup.

V_0 can be determined in the laboratory. In this prototype instrument, the calibrated V_0 was 98 ml.

C. Test 2 Results

In order to obtain more data, t_b was measured every 30 seconds in Test 2 following the same procedures of Test 1. The height of h_0 was set at 10 mm and the supply potential was set at -50 mm. I_0 can also be determined during the test. Test 2 was run on Oct. 10th, 1997. In this test, the volume of initial infiltration I_0 was 42 ml, and the infiltration data were shown in Appendix B and plotted in Fig. 8 and Fig. 9. In Fig. 9, it can be seen that the early time relationship was more linear if ignoring the start point.

D. Problems and Analysis

Before deriving the soil sorptivity, two assumptions should be made:

i) Assume equal amount of water i_0 infiltrate into two identical soils within different times t_0 and t_1 (Fig. 10), one (C_1) under a constant head Ψ_0 and another (C_2) starting at a later time, but under a falling head which will reach Ψ_0 at A and then remain constant. If t_0 is greater than t_1 by an appropriate amount, at A the soils will reach the same water content w_0.

ii) Two identical soils which possess the same water content and potential head will possess the same infiltration rate at any time.

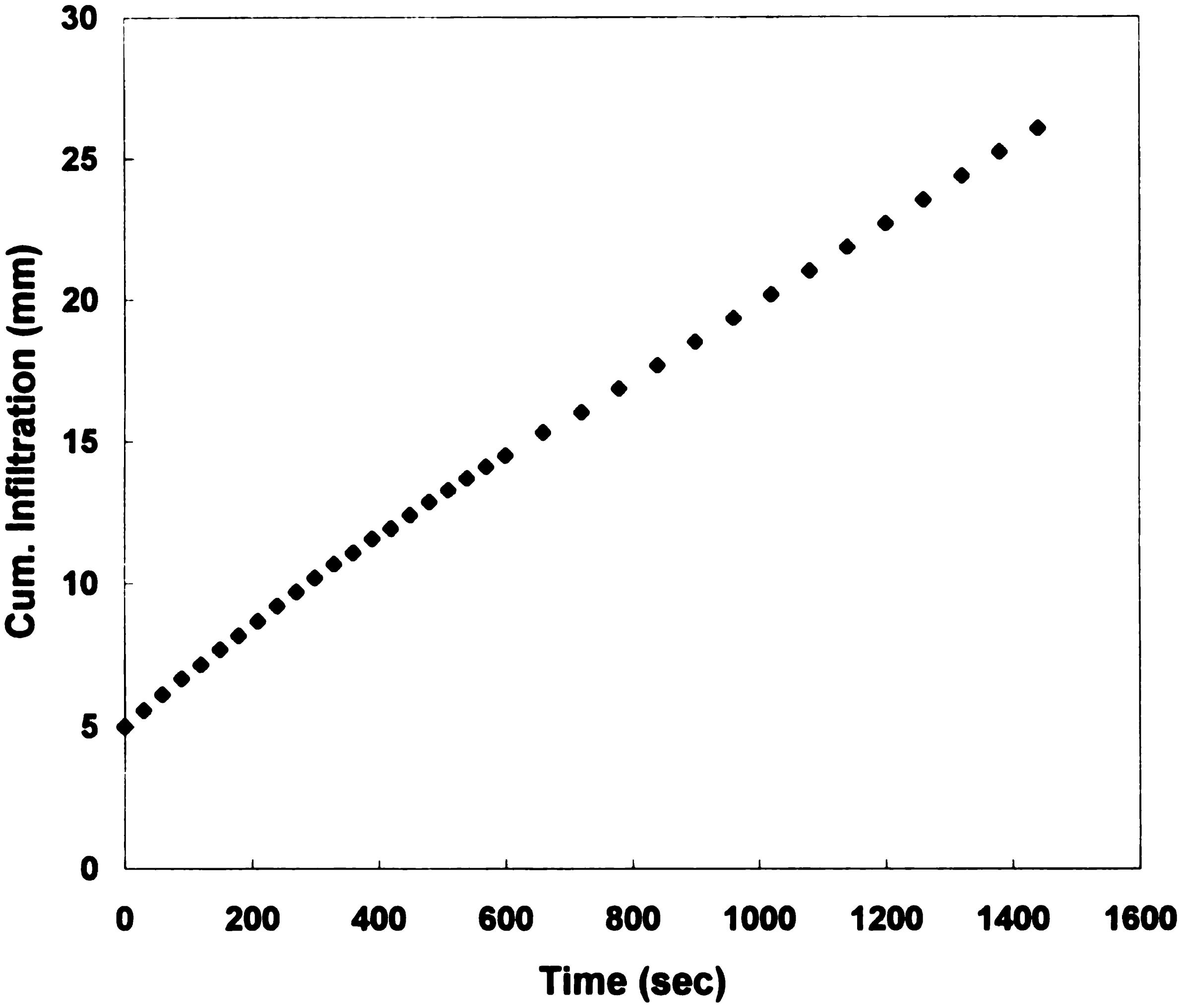

Figure 8. Cumulative infiltration vs. time diagram for Test 2.

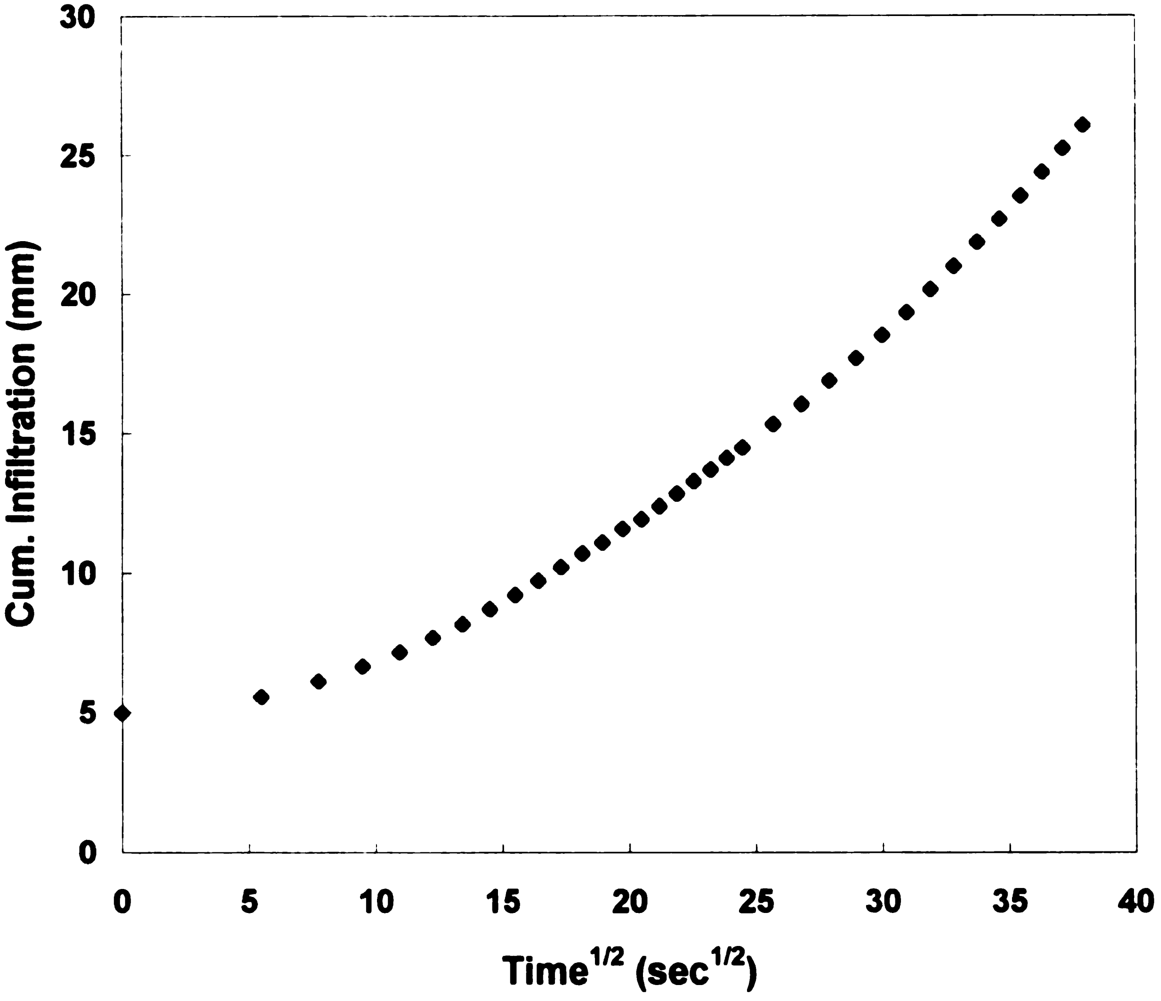

Figure 9. Cumulative infiltration vs. time$^{1/2}$ diagram for Test 2.

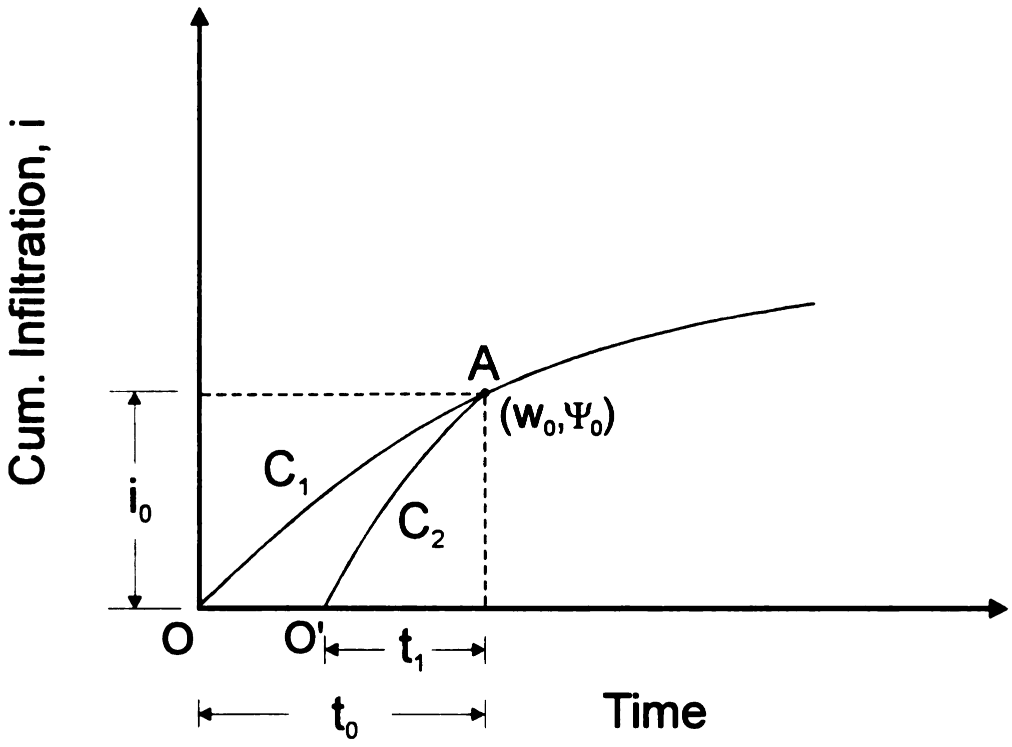

Figure 10. Cumulative infiltration vs. time diagram for constant head and falling head flow.

In Figure 11, C_1 is the curve of an ideal sorptivity flow measured with a constant supply potential Ψ_0 at any time. In fact, C_1 is an ideal curve because it is very difficult to design an non-electronic infiltrometer to set the supply potential to a desired value immediately at the start of the infiltration. The curve C_2 is from an experimental sorptivity flow which can be determined by the proposed infiltrometer. Once the experiment begins, the potential head of C_2 decreases during the water filling into the soil and reaches the desired potential Ψ_0 at A, at which time it remains constant and the air inlet tube starts bubbling. At A, both flows possess the initial infiltration i_0 and reach the same supply potential. According to the assumption, the curve C_1 and C_2 should meet at A, and thereafter C_1 and C_2 possess the same infiltration rate and can be considered identical. Within a short time increment dt, both have the same sorptivity which will be the slope of the straight line portion (Fig. 12),

$$S_0 = \frac{di}{(t_0 + dt)^{1/2} - t_0^{1/2}} \qquad (6)$$

where di is a small infiltration increment within dt. To determine S_0 from the experimental sorptivity flow, it is needed to measure t_0; however, t_0 is derived from the ideal sorptivity flow and cannot be measured by any available infiltrometer. The t_0 can be determined only when i_0 and S_0 are given, as expressed in the following equation,

$$t_0 = (i_0/S_0)^2 \qquad (7)$$

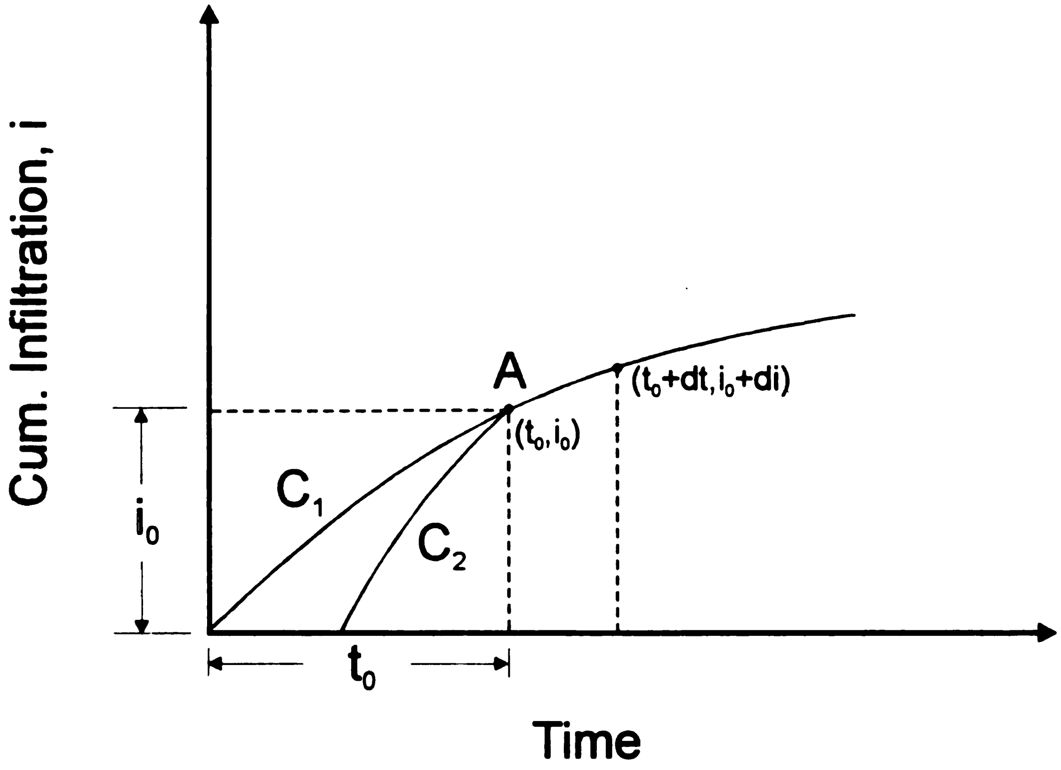
Cum. Infiltration, i
Time
A
(t_0, i_0)
(t_0+dt, i_0+di)
C_1
C_2
i_0
t_0

Figure 11. Cumulative infiltration vs. time diagram for ideal sorptivity flow and experimental sorptivity flow.

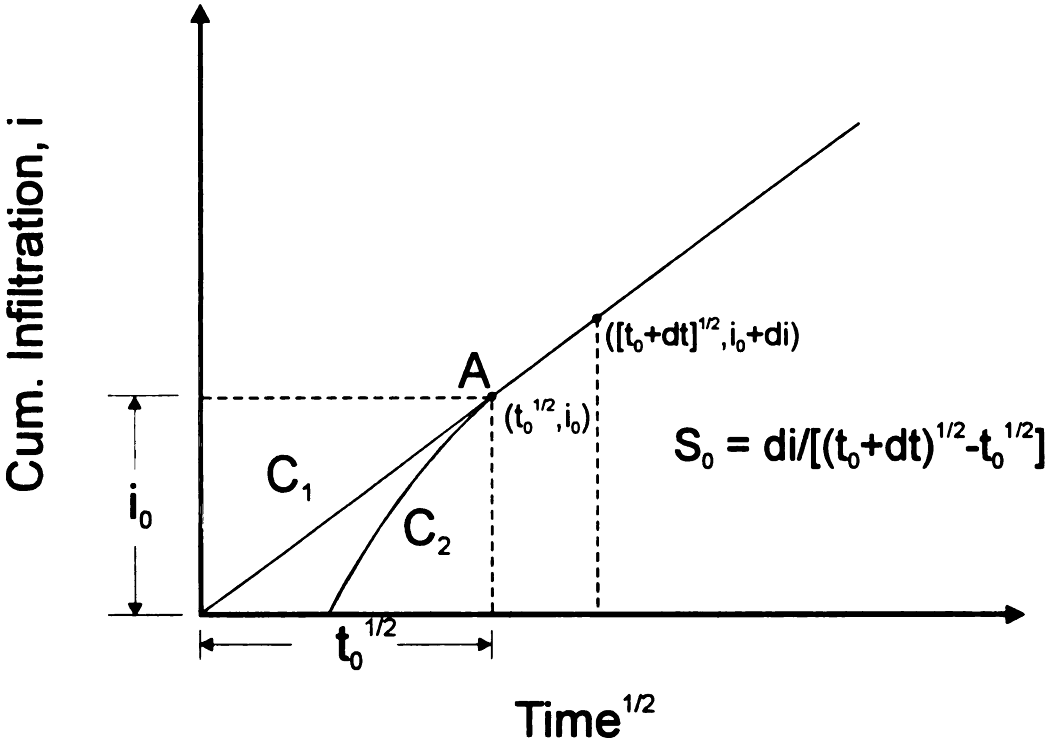
Cum. Infiltration, i
A
$(t_0^{1/2}, i_0)$
$([t_0+dt]^{1/2}, i_0+di)$
C_1
C_2
i_0
$t_0^{1/2}$
$S_0 = di/[(t_0+dt)^{1/2} - t_0^{1/2}]$
Time$^{1/2}$

Figure 12. Cumulative infiltration vs. time$^{1/2}$ diagram for ideal sorptivity flow and experimental sorptivity flow.

Since the measurement begins at A (whenever the supply potential reaches the desired value), t_0 would be the lag time between the start of the measurement and the ideal sorptivity flow. In the past, most researchers ignored t_0 (let $t_0 = 0$ in Eq.(6)) and derived the sorptivity as $di/dt^{1/2}$. This will result some errors in the sorptivity determination during the data analysis. Moreover, if the t_0 exceeds the duration of the sorptivity flow, the sorptivity phenomena ceases and can not be measured by the infiltrometer. In order to determine the correct sorptivity form the experimental data without measuring t_0, a conversion of the i vs. $t^{1/2}$ expression can be made to solve the above problem.

In Fig. 13, C_1 is the curve of an ideal sorptivity flow. C_2' is the coordinate shift of C_2 (Fig. 11). Thus C_1 and C_2' should be the identical flow after A and A'. According to Eq. (1), i is equal to $S_0t^{1/2}$. Therefore, by squaring both side of Eq. (1), i^2 can be expressed as S_0^2t. If the data are plotted with i^2 on the ordinate versus time on abscissa (Fig. 14), the slope of the straight line portion is the square of the sorptivity. Moreover, the sorptivity of C_1 and C_2' at any time can be expressed by

$$S_0^2 = \frac{(i_0 + di)^2 - i_0^2}{dt} \qquad \textbf{(8)}$$

The above derivation shows the sorptivity of an infiltration remains constant regardless of the start points. This result corresponds with

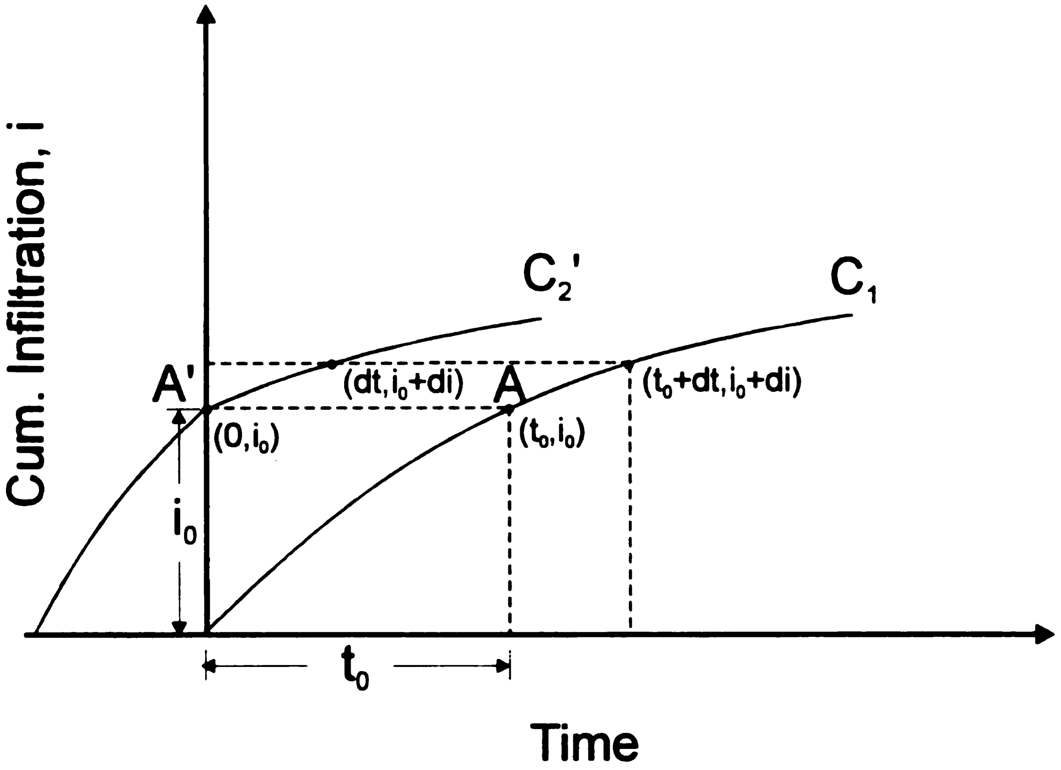
Cum. Infiltration, i
C2'
C1
A'
(dt,i0+di)
A
(t0+dt,i0+di)
(0,i0)
(t0,i0)
i0
t0
Time

Figure 13. Cumulative infiltration vs. time diagram for ideal sorptivity flow and experimental sorptivity flow with initial infiltration.

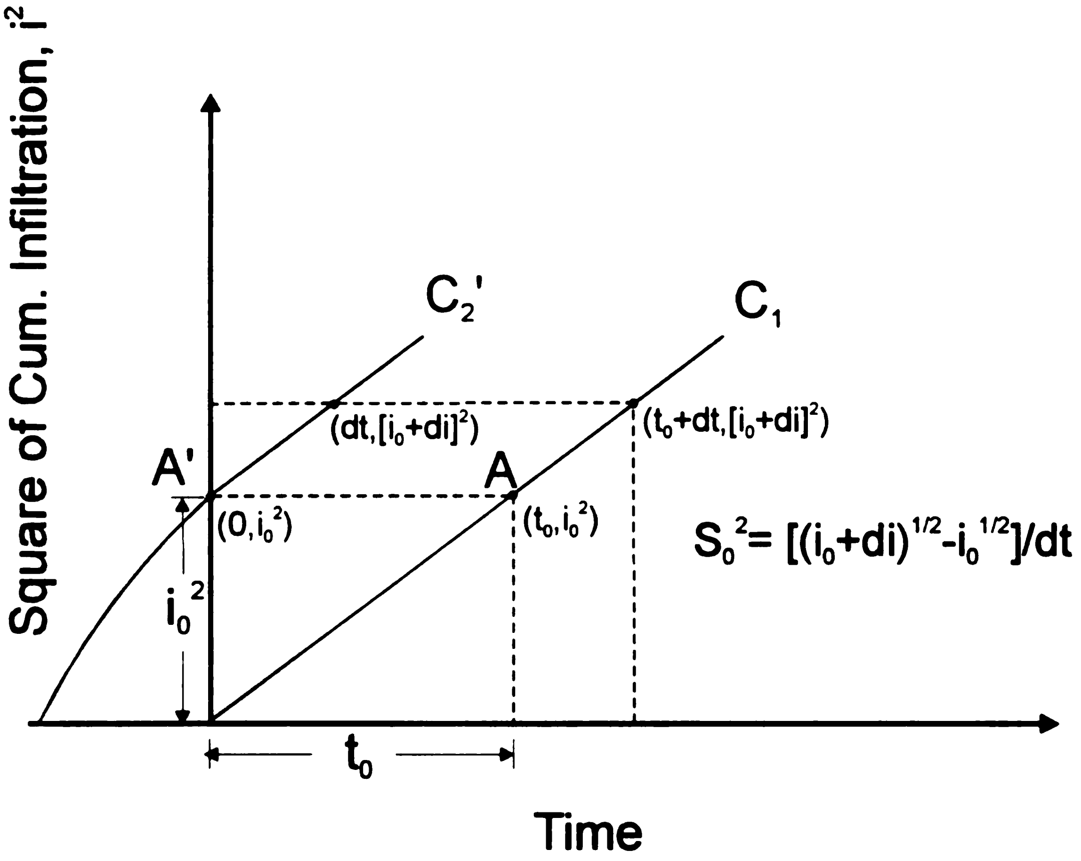
Square of Cum. Infiltration, i^2
C_2'
C_1
(dt,$[i_0+di]^2$)
(t_0+dt,$[i_0+di]^2$)
A'
A
(0,i_0^2)
(t_0,i_0^2)
i_0^2
$S_0^2 = [(i_0+di)^{1/2} - i_0^{1/2}]/dt$
t_0
Time

Figure 14. Square of cumulative infiltration vs. time diagram for ideal sorptivity flow and experimental sorptivity flow with initial infiltration.

the definition of the sorptivity. As a result, it is virtually impossible to avoid some initial infiltration during a sorptivity measurement. In order to determine the sorptivity from Eq. (8), it is necessary to measure the initial infiltration. Hopefully, it is much easier to evaluate i_0 in the field than t_0. Using this approach instead of the conventional i vs. $t^{1/2}$ diagram, the sorptivity can be determined correctly from the experimental data without measuring t_0.

E. Re-analysis of Test 2

The result of Test 2 was re-plotted in i^2 vs. time diagram and presented in Fig. 15. The slope of the straight line derived from the early time data was found to be 0.256. Therefore, the square of the sorptivity $S_0^2 = 0.256$ mm^2/sec and $S_0 = 0.506$ mm/sec$^{1/2}$. The t_0 can be calculated from Eq. (7) and was about 90 seconds. Since t_0 was short, the sorptivity flow would probably still happen within the regression range.

The straight line portion was determined by eye; however, a visual determination does not strongly influence the result. Table 2 shows the differences between the results of regression generated by different numbers of points. Using 2 points to 10 points, the deviation of the sorptivity is under 12% of the reading. This result shows that the determination of the straight line portion by eye would not cause intolerable error.

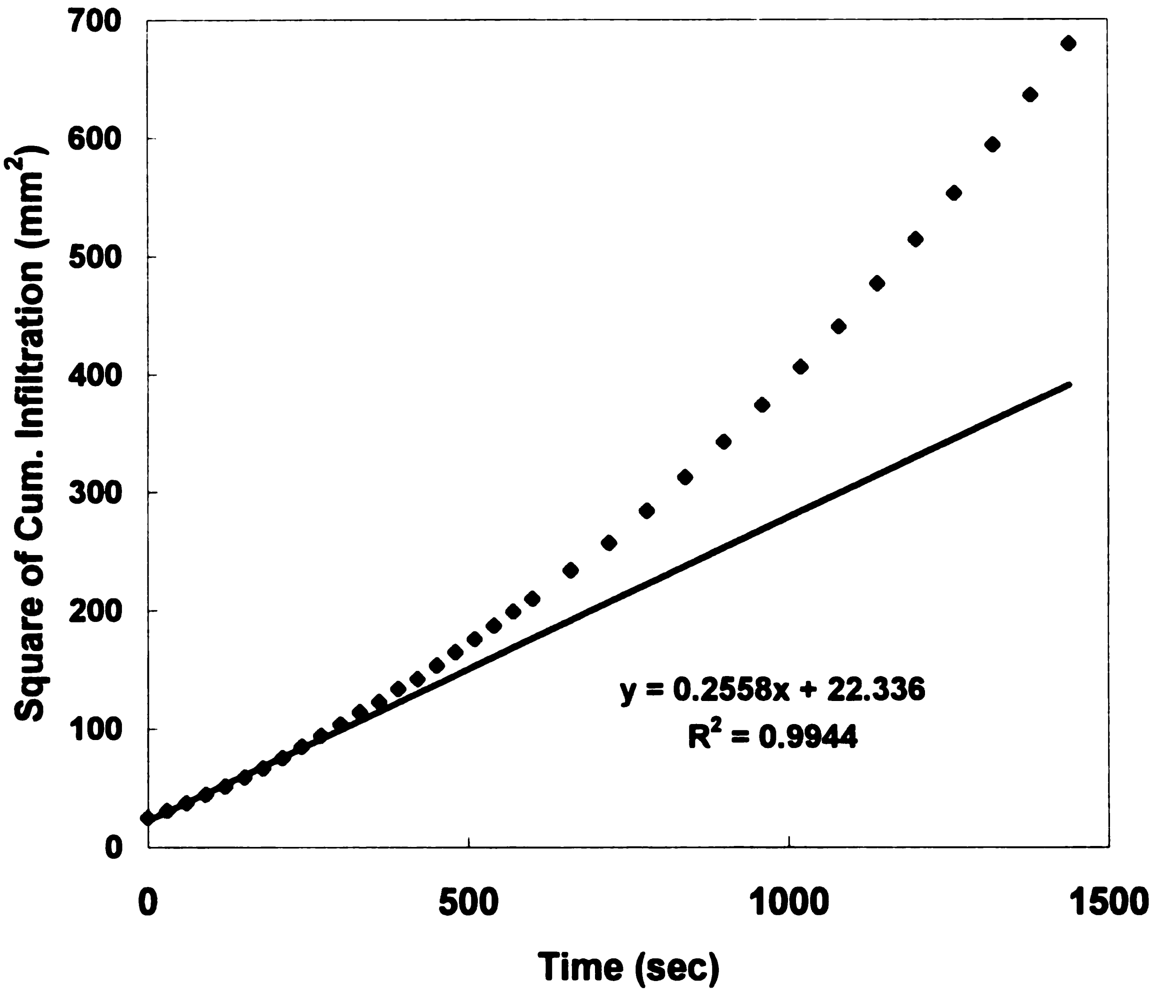

Figure 15. Cumulative infiltration^2 vs. time diagram for Test 2.

Table 2. Comparison of regression results generated by different numbers of points

NUMBERS OF POINTS	S^2 (mm^2/S)	R^2	S ($mm/S^{1/2}$)
2	0.198	1	0.445
3	0.207	0.9993	0.455
4	0.216	0.9987	0.464
5	0.220	0.9990	0.470
6	0.227	0.9983	0.476
7	0.233	0.9979	0.482
8	0.240	0.9969	0.490
9	0.248	0.9954	0.498
10	0.256	0.9944	0.506

VIII. Error Analysis

The velocity of the bubble is determined by its travel distance divided by its travel time. This was used to determine the velocity of the real flow in Test 1 and Test 2. The real flow is defined as the water flow minus the injected air bubbles into the flow meter. If the roughness of the tubing is very small, the movement of the bubble will be close to the real flow. The error analysis performed on the flow meter was mainly concerned with the relationship between the velocity of the injected bubbles and the real flow rate. This project was done in the laboratory in order to derive the empirical equations for the bubble movement and real flow for the field use.

A. Empirical Equation for Real Flow

The empirical equation for this project is defined by the following form:

$$Q = c_1 V_b^{C2} \qquad (9)$$

Where:

Q = discharge of real flow

V_b = velocity of injected bubble

c_1, c_2 = constants from the regression

The volume of each injected bubble was assigned 0.1 ml which is corresponding to the field use.

B. Experiment Design

Basing on the empirical equation, the schematic diagram of the designed system to be used for this experiment is shown in Fig. 16. The flow rate is varied by changing the water level in the water reservoir. A hypodermic needle was used to inject 0.1 ml air bubble into the flow meter (3.2 mm I. D.). The velocity of the bubble is calculated by measuring its travel distance and travel time. A digital scale with a pan on it was located at the end of the flow meter. By measuring the outflow within a certain time the flow rate of real flow can be determined. Since the size of the water reservoir (about 209 mm I. D.) is comparatively large, within a short time increment, the pressure head and the flow rate remain constant.

C. Regressions and Results

The experiment was done in the laboratory at about 15 °C of water temperature which was the most common condition in the field tests. The experimental data is shown in appendix C. By plotting the Q vs. V_b in logarithmic scale (Fig. 17) The slope of the straight line is found to be c_1, and the interception is found to be log c_2. The regression equation can then be determined as follows:

$$Q = 4.647\ V_b^{\ 0.9331} \qquad \textbf{(10)}$$

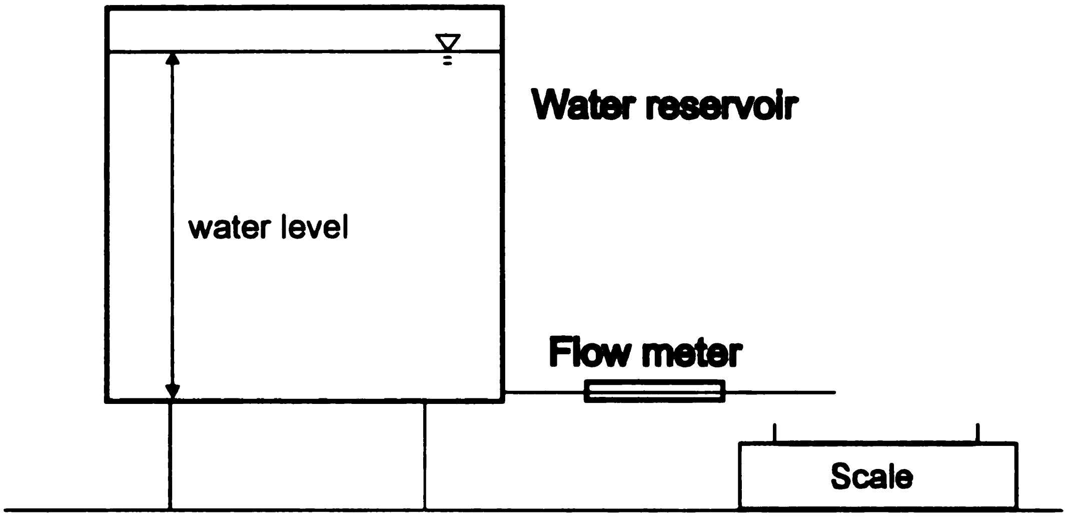
Water reservoir
water level
Flow meter
Scale

Figure 16. Designed system for error analysis.

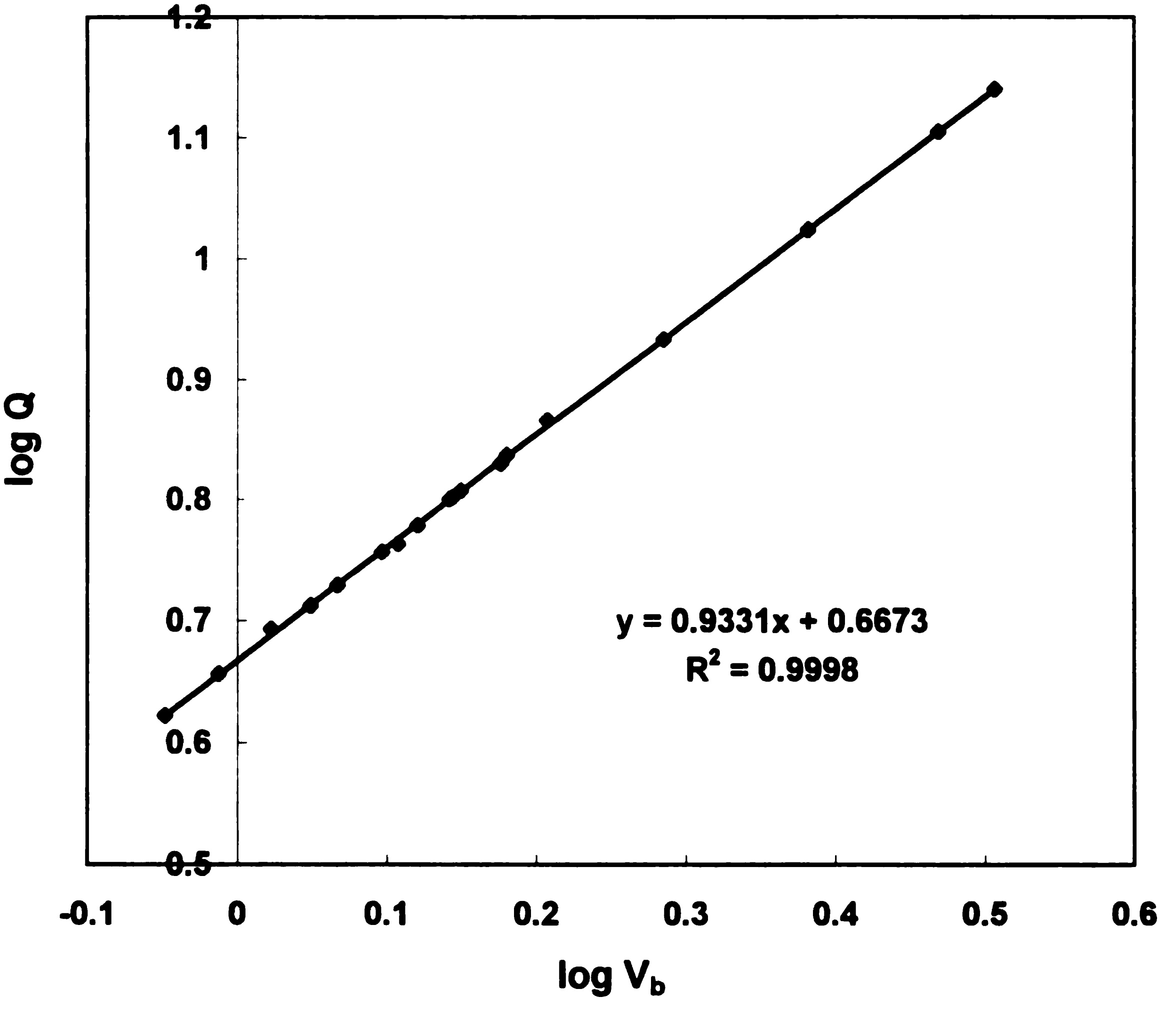

Figure 17. Regression curve for the result of error analysis.

The r^2 for the regression curve is 0.9998 which provides a strong confidence for the result of the regression. The unit of Q is milliliters per minute and while the unit of V_b is centimeters per second. The operation range of the empirical equation was from 3 ml/min to 15 ml/min. The Eq. (10) can be easily used to estimate the real flow by using the flow meter in the field.

E. Discussions

The empirical equation was derived from the experimental data by simulating the field condition in the laboratory. Eq. (10) provide an accurate means to determined the discharge of a small flow. According to the experiment, the original mean square error was 0.32 ml^2/min^2, and was reduced to 0.001 ml^2/min^2 by applying Eq. (10) to predict the real flow. This result provides more accuracy than just using the bubble velocity to represent the velocity of the real flow. The operation ranges for the Eq. (10) is from 3 ml/min to 15 ml/min which is the most common range for the sorptivity flow of sand and loam. For very clayey soil, the infiltration rate is much smaller than 3 ml/min and can not be simulated in laboratory; therefore, the velocity of the bubble is used to represent the velocity of real flow. Even under these conditions, the flow meter is still an easy way to estimate this kind of flow. This analysis shows that the flow meter can be possibly applied in many different fields especially when the flow is slow and can not be determined by any other methods.

IX. Test System II

According to the derivation in the previous paragraphs, the sorptivity is able to be estimated accurately in i^2 vs. t diagram. Moreover, the Eq. (10) provides more accuracy to predict the real flow by the bubble velocity. The designed infiltrometer was applied on three different soil textures in order to test its operation ranges. Two tests were performed on Capac loam and three tests were done on Riddles-Hillsdale sandy loam and Granby loamy fine sand. Each test was tested under different supply potentials.

A. Results for Site 1

At site 1, two tests were conducted on Capac loam. The experiments were operated under different supply potential, Ψ_0, on October 19th, 1997 at the Michigan State University research farm at East Lansing. The data are shown in Appendix B and plotted in Fig. 18 and Fig. 19 The slope of the straight line in Fig. 18 and Fig. 19 is the square of sorptivity for the field soil. The results for each test are shown in tabular form in Table 3. The duration for both tests was over 80 minutes. The sorptivity of the first test was 0.401 mm/min$^{1/2}$ and the sorptivity of the second test was higher and was 0.362 mm/min$^{1/2}$. The V_{total} is the volume of the total infiltration which can be determined by observing the differential between the initial and finial weight on the

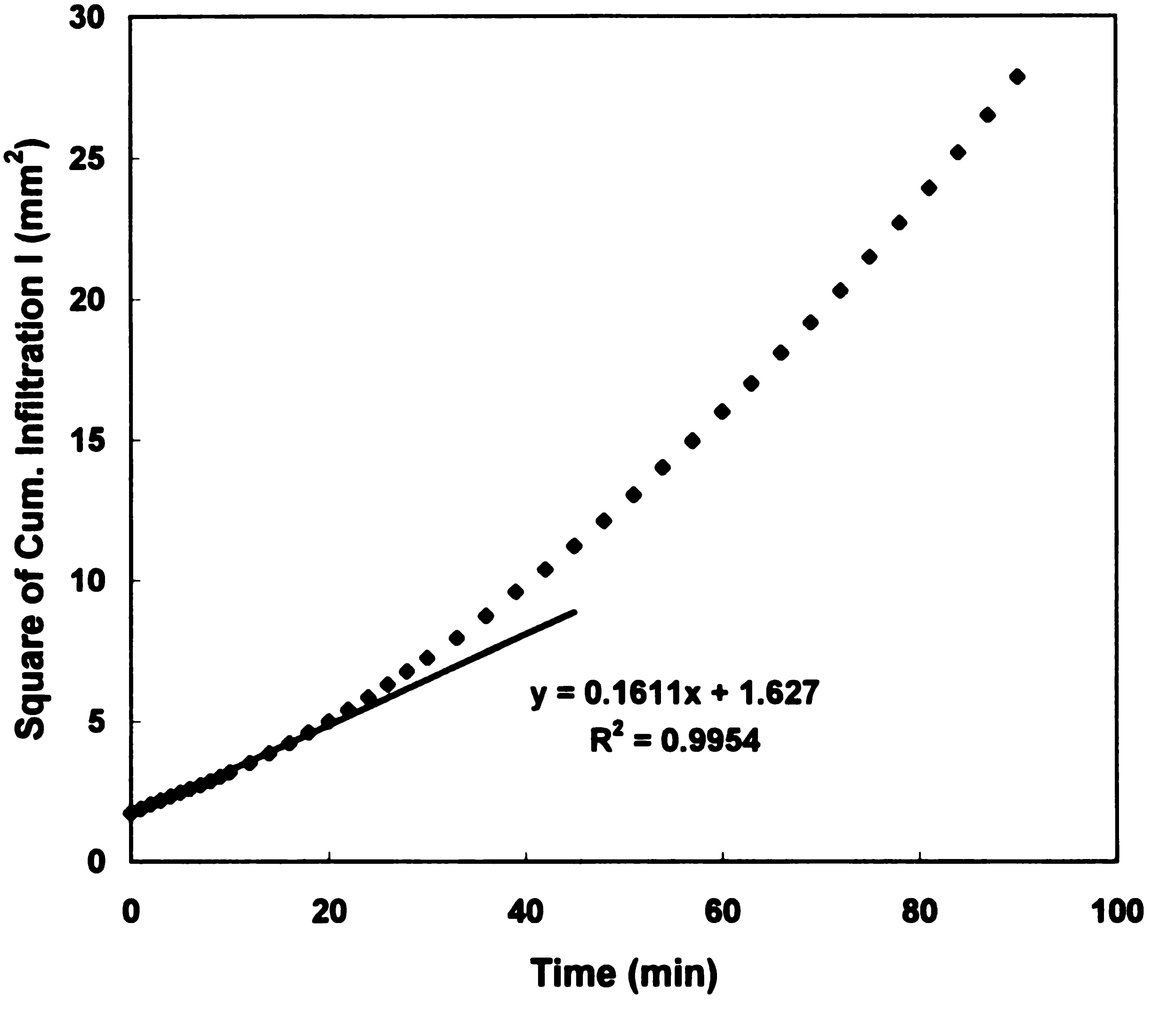

Figure 18. Result of the first test for Capac loam.

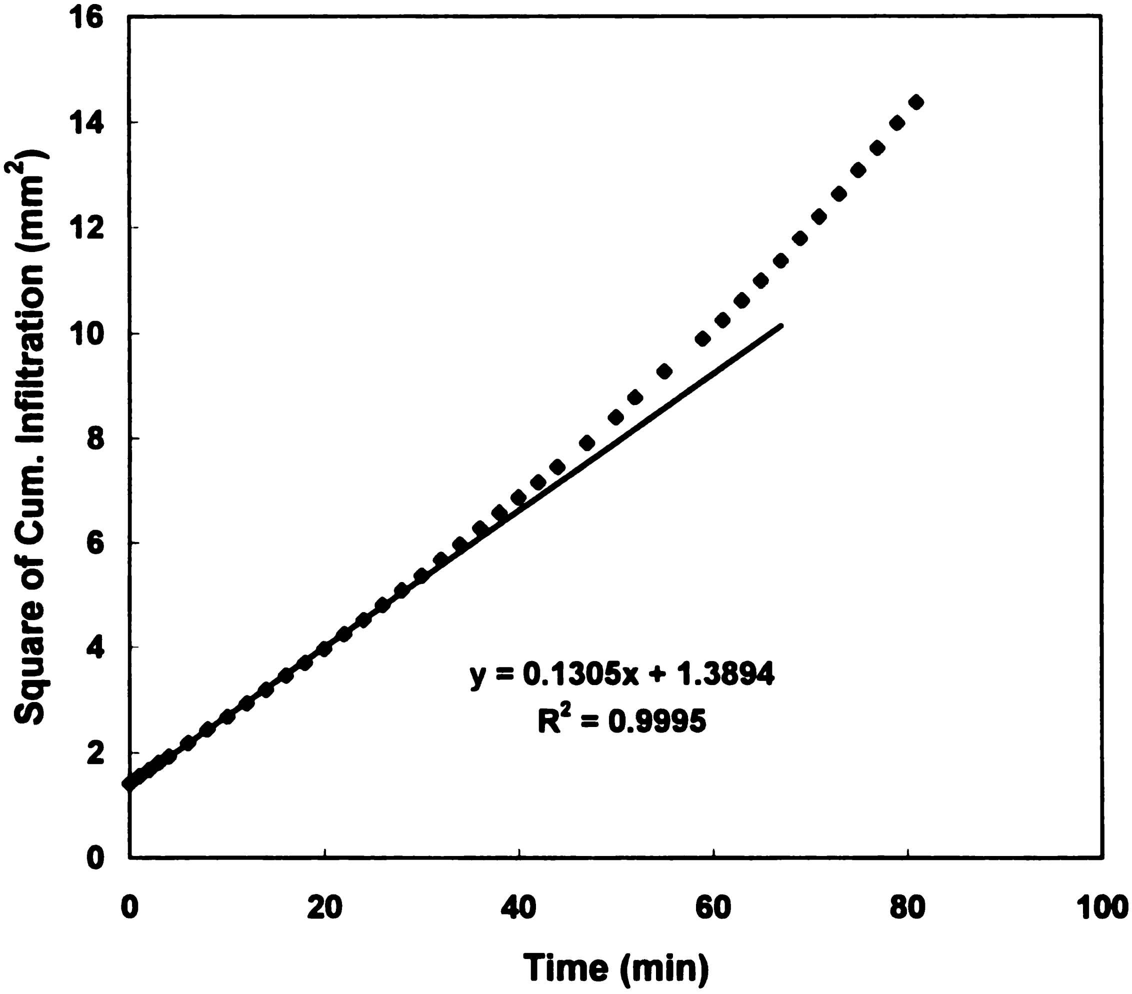

Figure 19. Result of the second test for Capac loam.

digital scale during the infiltration. The V_{total} can also be estimated by the flow meter and would be the total amount of the cumulative infiltration. In both tests, the V_{total} determined by the flow meter was close to the V_{total} determined by the scale. This result shows no intolerable error happened during the tests.

Table 3. Comparison of results from different tests at site 1.

No.	Tension Ψ_0	I_0 (ml)	S^2 (mm^2/min)	S ($mm/min^{1/2}$)	V_{total} by scale	V_{total} by flow meter	t_0 (min)
1	-10 mm	11	0.161	0.401	44 ml	44.4 ml	10.63
2	-30 mm	10	0.131	0.362	32 ml	31.2 ml	10.78

B. Results for Site 2

At site 2, three tests were conducted on Riddles-Hillsdale sandy loam. The tests were operated on November 9th, 1997 at the research farm on university property at East Lansing. The data are shown in Appendix B and plotted in Fig. 20 to Fig. 22. The results for each test are shown in Table 4. The operation time for all three tests was 40 minutes. The sorptivity of the first test (Fig. 20) was 0.282 $mm/sec^{1/2}$, and the sorptivity of the second test (Fig. 21) was 0.260 $mm/sec^{1/2}$. The sorptivity of the third test (Fig. 22) was 0.239 $mm/sec^{1/2}$. The lag time t_0 for each test was around 2 minutes. For all three tests, the difference between the V_{total} determined by the flow meter and V_{total} determined by the scale was less than 3% of total infiltration.

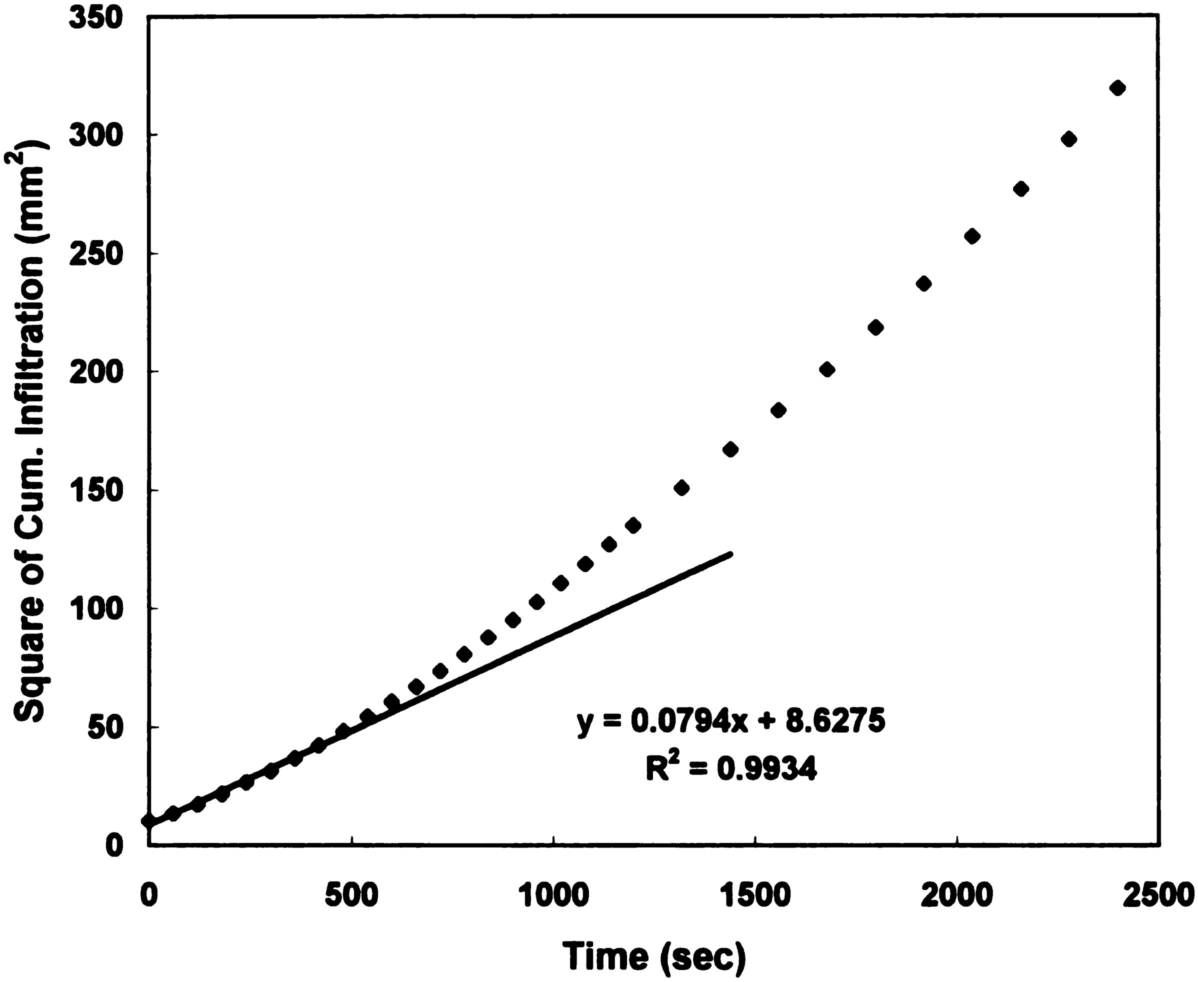

Figure 20. Result of the first test for Riddles-Hillsdale sandy loam.

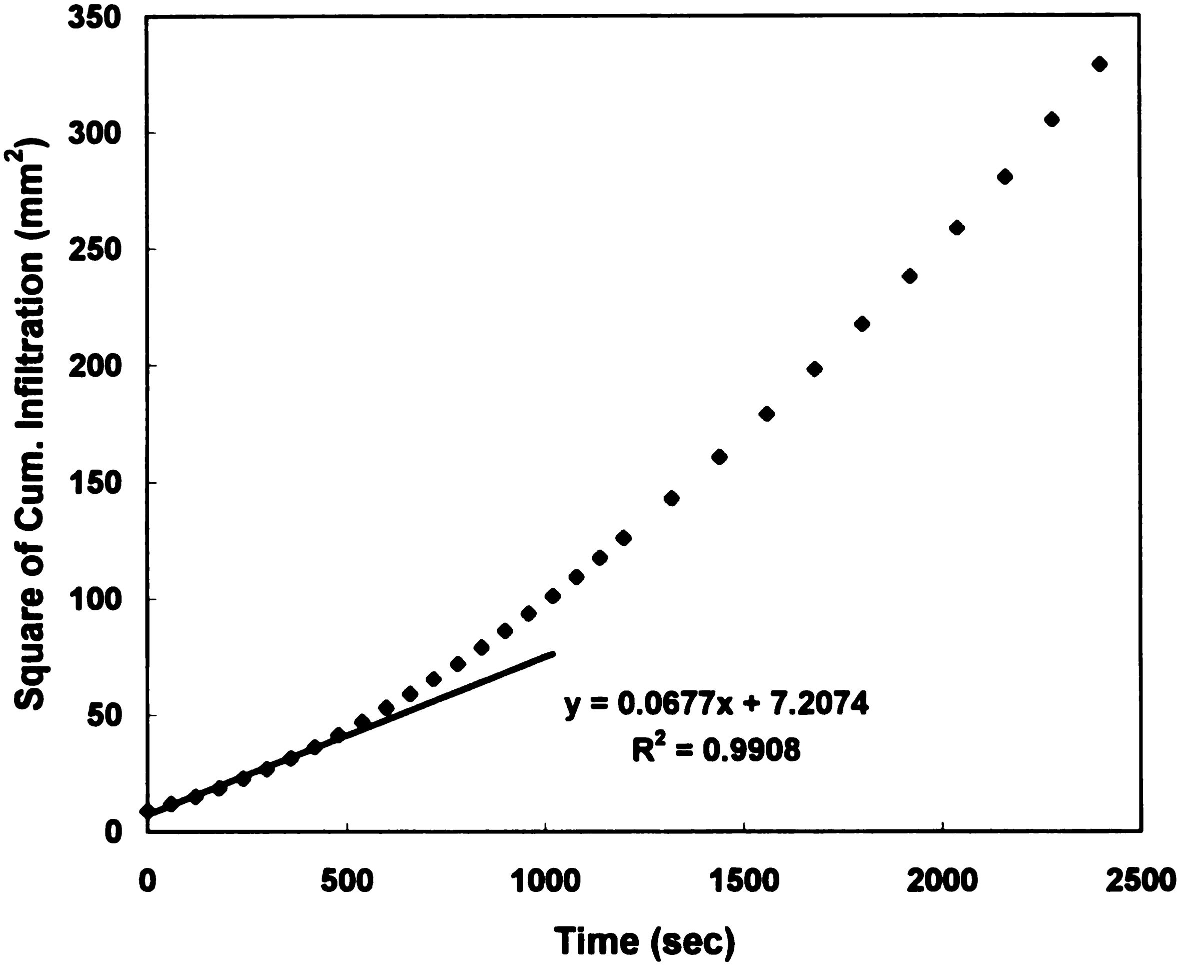

Figure 21. Result of the second test for Riddles-Hillsdale sandy loam.

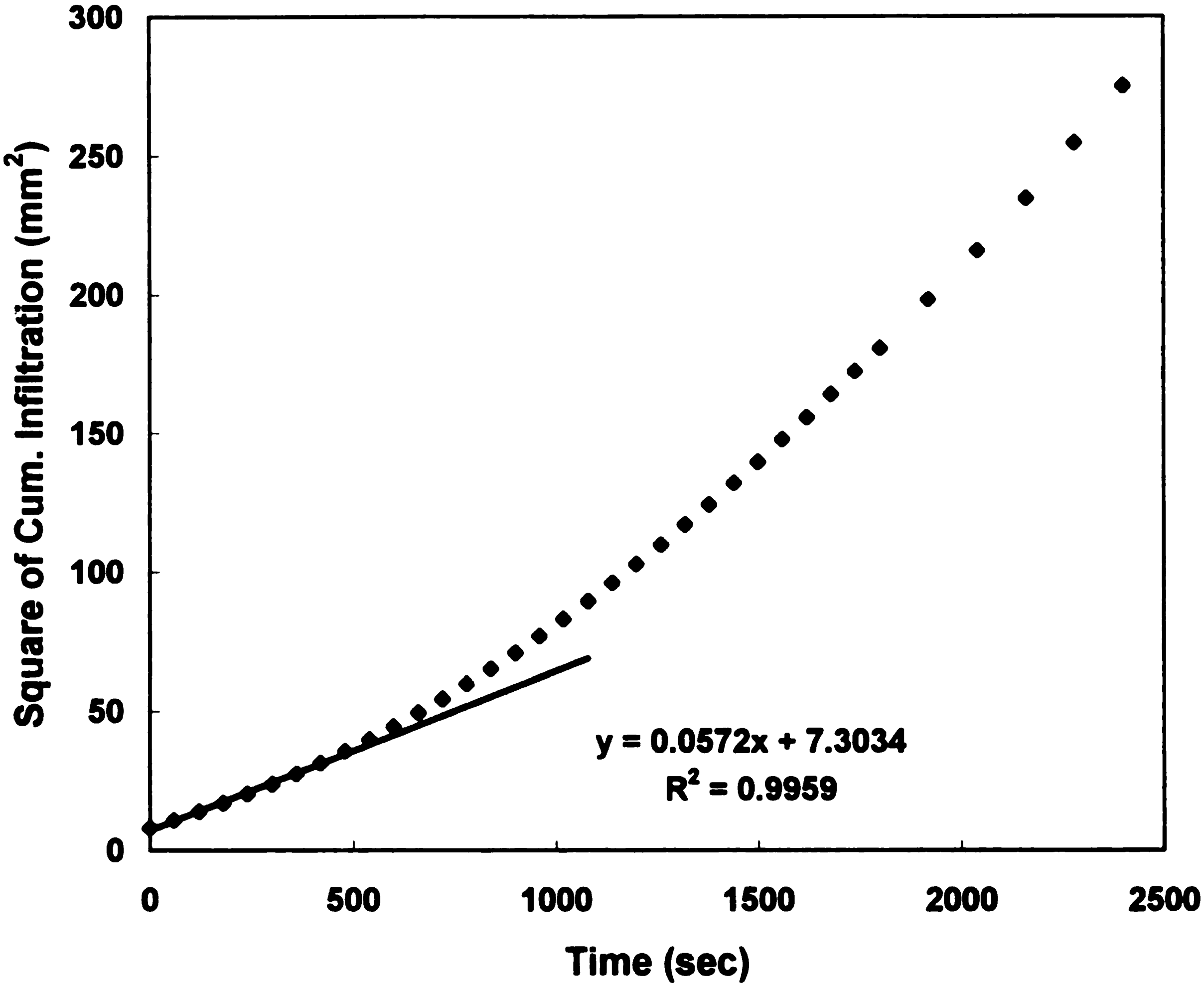

Figure 22. Result of the thired test for Riddles-Hillsdale sandy loam.

Table 4. Comparison of results from different tests at site 2.

No.	Tension Ψ_0	I_0 (ml)	S^2 (mm^2/sec)	S ($mm/sec^{1/2}$)	V_{total} by scale	V_{total} by flow meter	t_0 (sec)
1	-10 mm	27	0.0794	0.282	152 ml	150.4 ml	129.5
2	-30 mm	25	0.0677	0.260	154 ml	152.6 ml	130.6
3	-50 mm	24	0.0572	0.239	142 ml	139.6 ml	142.4

C. Results for Site 3

At site 3, three tests were conducted on Granby loamy fine sand. The tests were operated on November 14th, 1997 at the research farm on university property at East Lansing. The data are shown in Appendix B and plotted in Fig. 23 to Fig. 25. The operation time for all three tests was 30 minutes. The sorptivity of the first test (Fig. 23) was 0.480 mm/sec$^{1/2}$, and the sorptivity of the second test (Fig. 24) was 0.473 mm/sec$^{1/2}$. The sorptivity of the third test (Fig. 25) was 0.409 mm/sec$^{1/2}$. For the third test, t_0 increased to 97 seconds because the infiltrometer needed more time to reach the higher supply potential. For all three tests, the difference between the V_{total} determined by the flow meter and V_{total} determined by the scale was less than 3% of total infiltration. The results for each test are shown in table 5.

Table 5. Comparison of results from different tests at site 3.

No.	Tension Ψ_0	I_0 (ml)	S^2 (mm^2/sec)	S ($mm/msec^{/2}$)	V_{total} by scale	V_{total} by flow meter	t_0 (min)
1	-20 mm	28	0.231	0.480	304 ml	301 ml	49
2	-40 mm	30	0.224	0.473	296 ml	293 ml	57
3	-80 mm	34	0.167	0.409	232 ml	231 ml	97

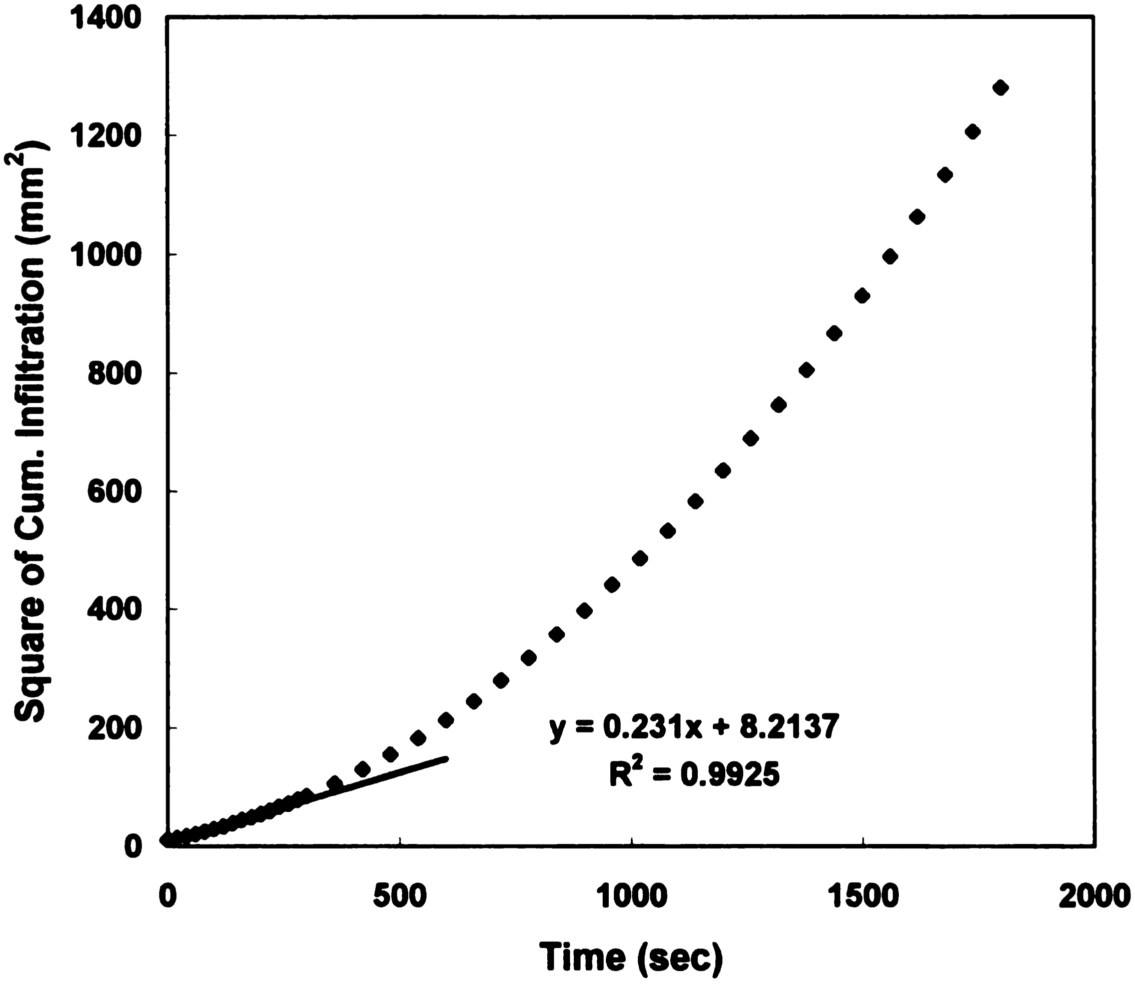

Figure 23. Result of the first test for Granby loamy fine sand.

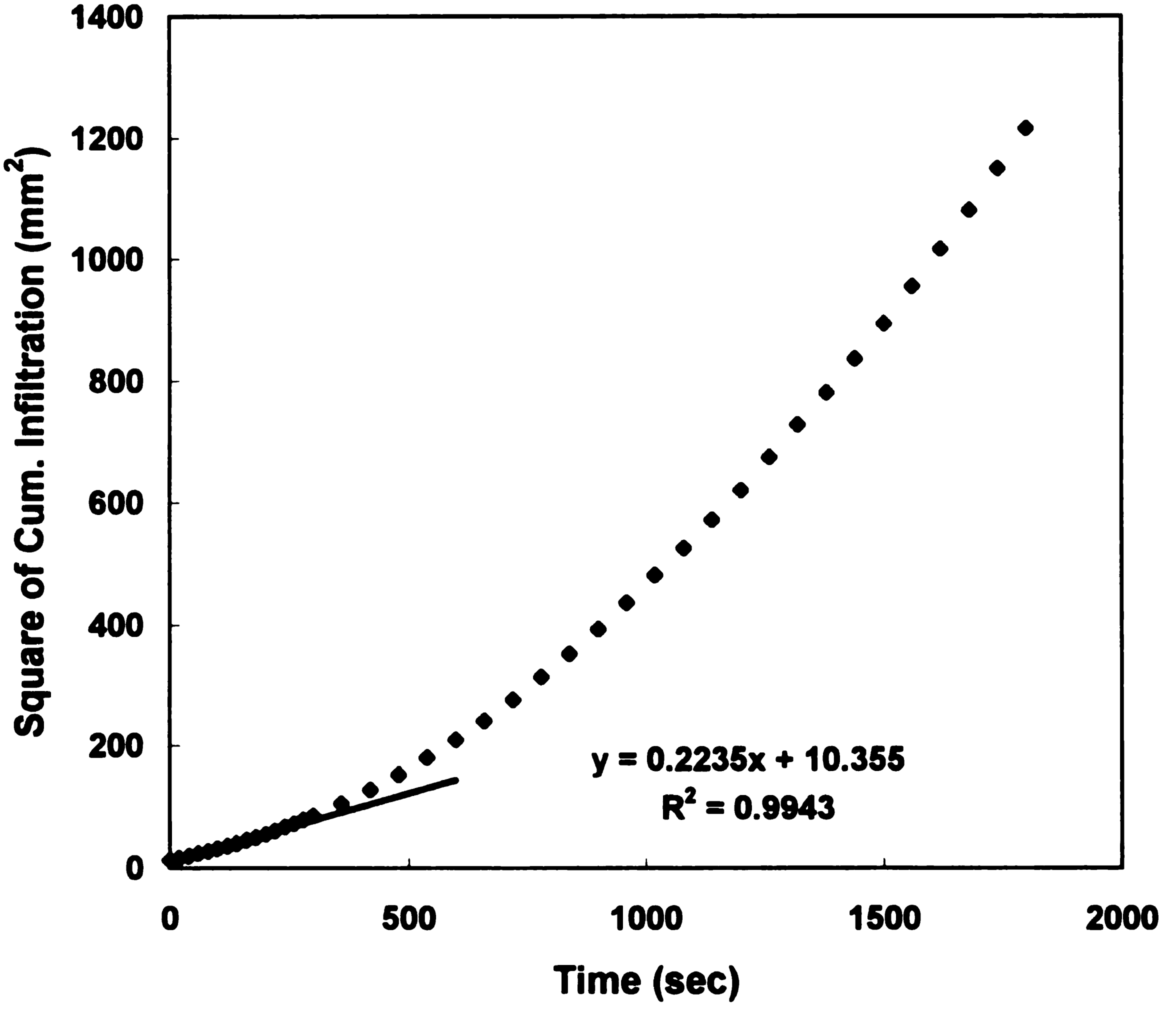

Figure 24. Result of the second test for Granby loamy fine sand.

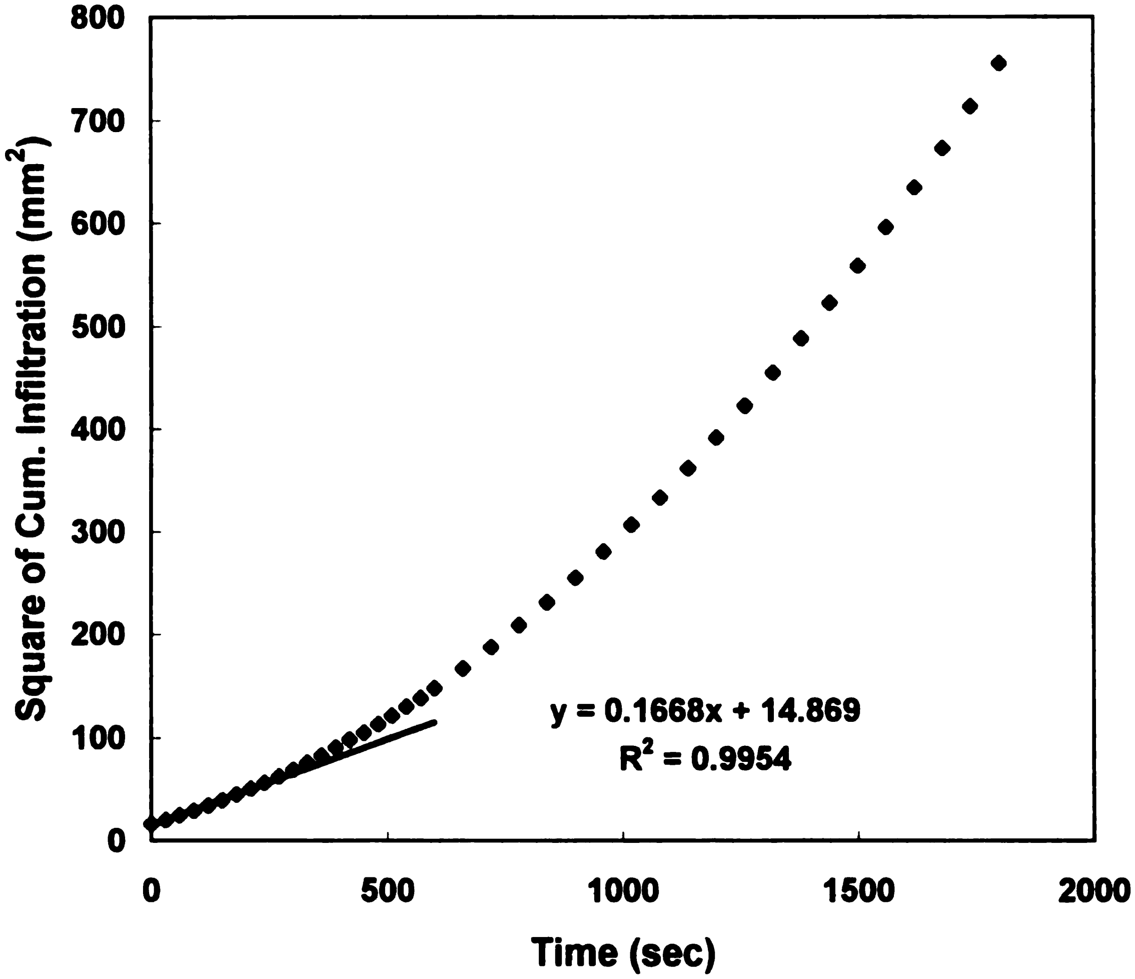

Figure 25. Result of the third test for Granby loamy fine sand.

In addition to the sorptivity, the macroscopic capillary length λ_c and the hydraulic conductivity can also be determined by applying Eq.s (2) and (4). The initial water content θ_{dry} and final water content θ_{wet} were measured during the tests and shown in Table 6. The steady state flow rate $Q/\pi r^2$ is found by plotting the cumulative infiltration during the last part of the infiltration as a function of time. The plot should be linear at large time. The slope of this line is the steady state flow rate $Q/\pi r^2$. The plots are shown in Fig. 26 to Fig. 28 and the results are shown in Table 6. The soil hydraulic conductivity at -20 mm supply potential was 17 mm/hr, at -40 mm was 14 mm/hr, and at -80 mm was 11.8mm/hr. The macroscopic capillary length for each test was 110 mm, 108 mm, and 118 mm. For many field soils λ_c is close to 100 mm (White and Sully, 1987), so the results were consistent to the field situation.

Table 6. Comparison of results from different tests at site 3.

No.	Tension Ψ_0	S (mm/sec$^{1/2}$)	$Q/\pi r^2$ (mm/sec)	θ_{dry}	θ_{wet}	K_0 (mm/hr)	λ_c (mm)
1	-20 mm	0.480	0.0176	0.05	0.292	17	110
2	-40 mm	0.473	0.0165	0.05	0.290	14	108
3	-80 mm	0.409	0.0128	0.05	0.287	11.8	118

D. Discussions

According the results, the soil had higher sorptivity under less supply potential in each site. This outcome is consistent to the field situation, since the higher negative supply potential would restrict the

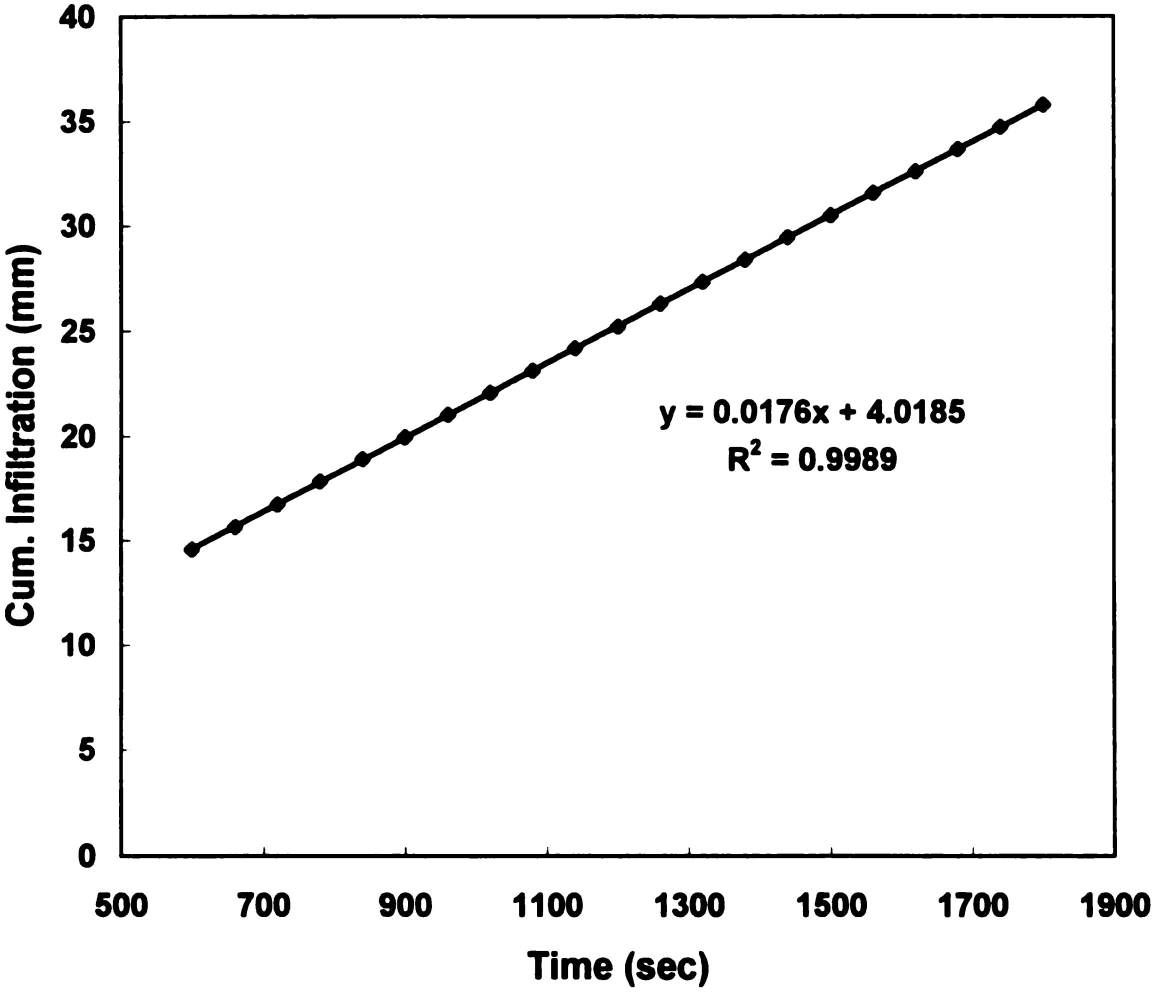

Figure 26. Result of steady state flow for the first test at site 3.

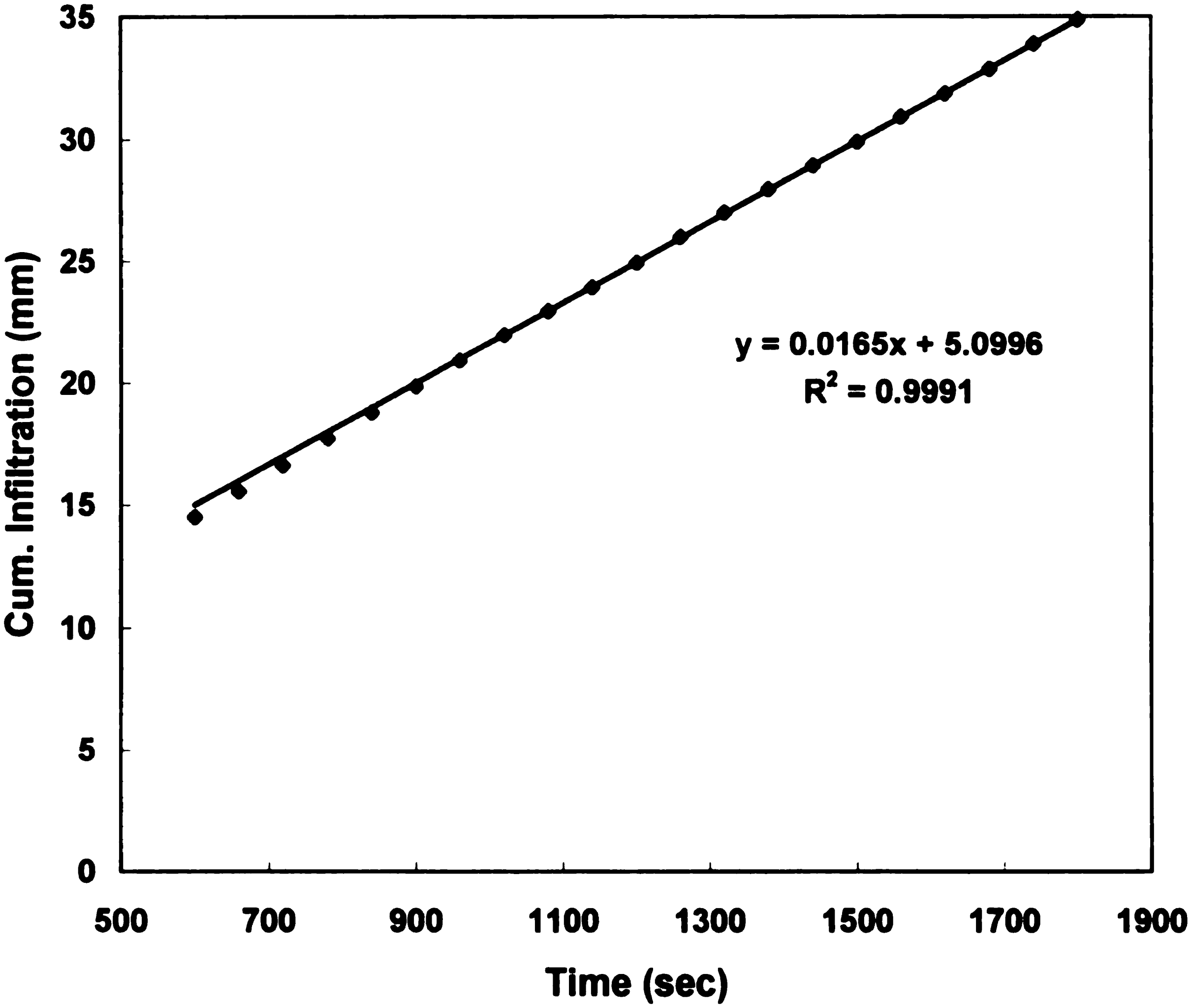

Figure 27. Result of steady state flow for the second test at site 3.

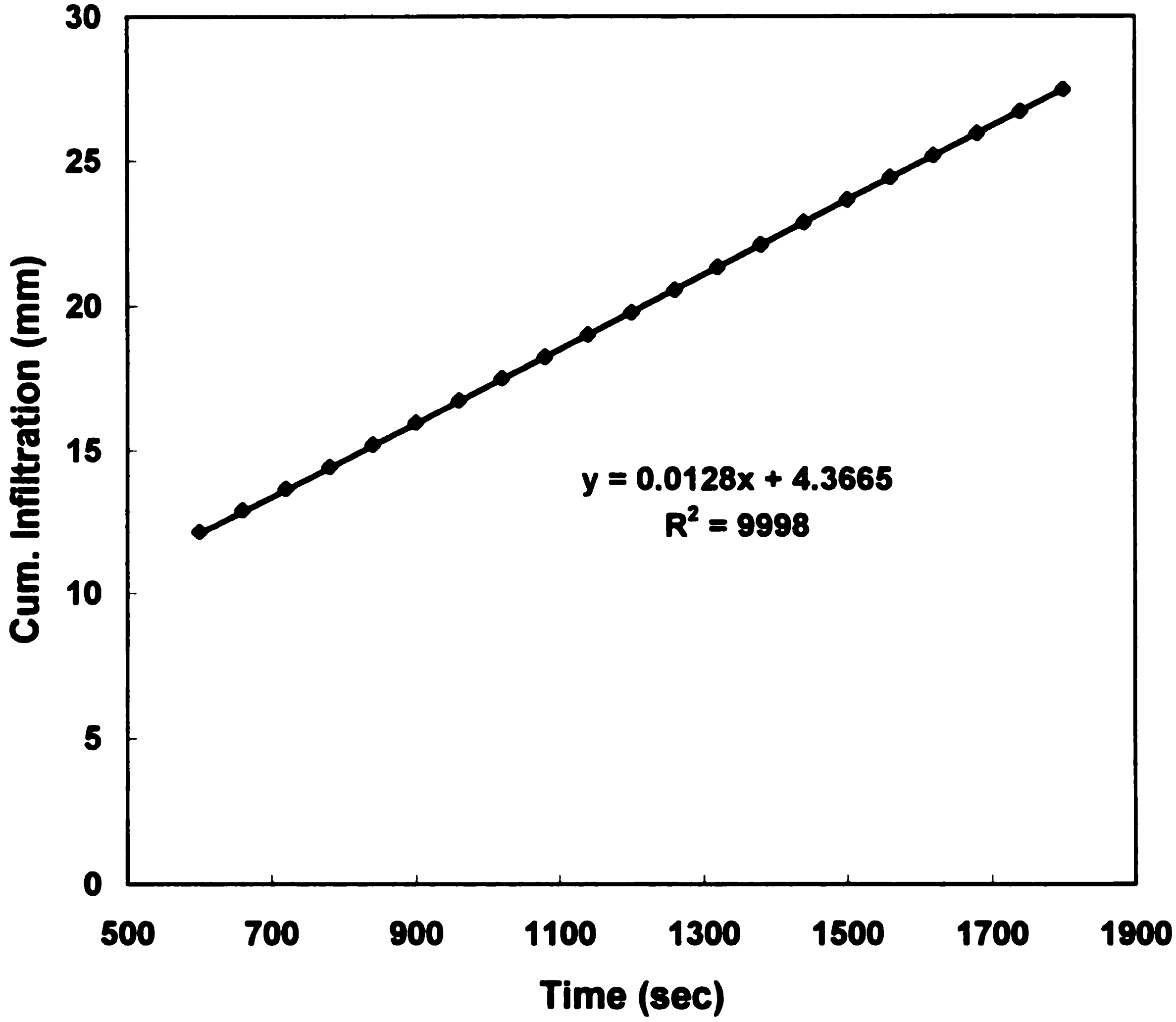

Figure 28. Result of steady state flow for the third test at site 3.

soil to absorb water from the surface.

In site 3, the soil hydraulic conductivity for each test was much smaller than the steady state flow rate, $Q/\pi r^2$. This result demonstrates the fact that the soil absorption dominated the infiltration when the soil infiltration is operated under some negative supply potential.

The difference between the V_{total} determined by the flow meter and V_{total} determined by the scale was considered as a parameter, ΔV_{total}, to examine the accuracy of each test. For all the tests, the ΔV_{total} was less than 3% of the total infiltration. This result verifies the high accuracy of the designed flow meter and shows using the flow meter to estimate a small infiltration is a feasible and accurate device.

The t_0 is an important parameter in sorptivity measurement, since if the t_0 is greater than the duration of the sorptivity flow, the measured sorptivity can not represent the true characteristic of the tested soil. In site 1, the t_0 for each test was about 10 minutes. By field experiences, the duration of the sorptivity flow for Capac loam was over 30 minutes; therefore, the sorptivity flow was possibly still taking place, since t_0 for both tests was much less than 30 minutes. In site 2, the t_0 for each test was around 2 minutes. According to the field experiences, the duration of the sorptivity flow for Riddles-Hillsdale sandy loam would hold over 5 minutes which is greater than t_0 of all three tests in site 2. Therefore, the sorptivity flows were assure to happen. In site 3, the t_0 for each test was around 1 to 1.5

minutes which should be small enough to assure the proceeding of the sorptivity flow.

For the first test in site 1, the soil sorptivity was 0.401 mm/hr$^{1/2}$ when the volume of initial infiltration, I_0, was equal to 11 ml. However, the sorptivity would decrease to 0.204 mm/hr$^{1/2}$ by omitting the initial infiltration (let $i_0 = 0$). Therefore, even 11 ml of initial infiltration would possibly create 100% of error in the sorptivity determination. This shows the volume of initial infiltration, I_0, is another important parameter which needs to be decided in sorptivity measurement especially for clayey soil.

According to the field experiences, the operation range of the flow meter was from 1 ml/min to 20 ml/min. Within this range, the flow rate was able to be determined accurately and conveniently by the flow meter. For some tests done in clay, the infiltration rate was much smaller than 1 ml/min and was not able to be measured by this device.

X. Recommendations

There are several suggestions that would improve the system but have not been tested. In the first version of the designed infiltrometer, some problems related to the determination of the initial infiltration and the flow rate were discovered. The first was matching the operation range of flow meter with the infiltration rate of soils. As mentioned before, the applicable range of the flow meter was from 1 ml/min to 20 ml/min, however, the infiltration rate of some clays was under this range. This means the flow meter can not measure such a small flow accurately. The flow rate is relative to the cross sectional area of the sample cup. Since this was a prototype version of the system, the size of the sample cup was determined to be adequate for field tests and no further attempts were made to correct the problem.

In order to create the flow, a bigger sample cup is necessary to be applied. A 200 mm I. D. and 50 mm length sample cup is suggested to be used in the future for clay. By using the suggested sample cup, the flow can increase to as much as about four times than the prototype. For clay, the 50 mm length cup should be long enough to assure the proceeding of the one dimensional flow within the sample cup during the early infiltration. The top of the sample cup should be still detachable as the prototype for convenient installation.

The second problem encountered was the calibrated volume of the upper room in the sample cup, V_0 (Fig. 7). The accuracy of the V_0 would hugely influence the result of I_0, volume of the initial infiltration. Since in the previous tests, V_0 was forced to desired value by filling dry fine sand on the soil surface, it was difficult to set V_0 accurately by this method. A detachable metal plate with 1 mm pores (Fig. 29) is suggested to fixed at a desired position in the sample cup to solve this problem. According to Clothier and White (1981), pores having a diameter over 0.76 mm will not affect infiltration of water. Beneath the porous plate, a thin layer of dry fine sand was used to ensure good contact between the plate and the field soil without influencing the sorptivity flow (Clothier and White, 1981). By adding the porous plate in the sample cup, V_0 will be constant, and both V_0 and I_0 can be calibrated more accurately.

Furthermore, the determination of the amount of the initial infiltration I_0 was another problem needed to be solved. In the prototype, the I_0 was measured by a digital scale which is much more expensive than the infiltrometer. To reduce the cost of this project, some modifications are suggested to be done on the water reservoir. In Fig. 30, a 38 mm I. D. and 150 mm length tube is added on the prototype. The adding tube should be made by clear material and have scales on the wall in order to observe the water level. By recording the differences between the height of water surface, the volume of the initial infiltration I_0 can be determined easily. The advantages of this two sectional tube design are: i) lower cost for the determination of I_0 than prototype, ii) contain more water for long term experiment than

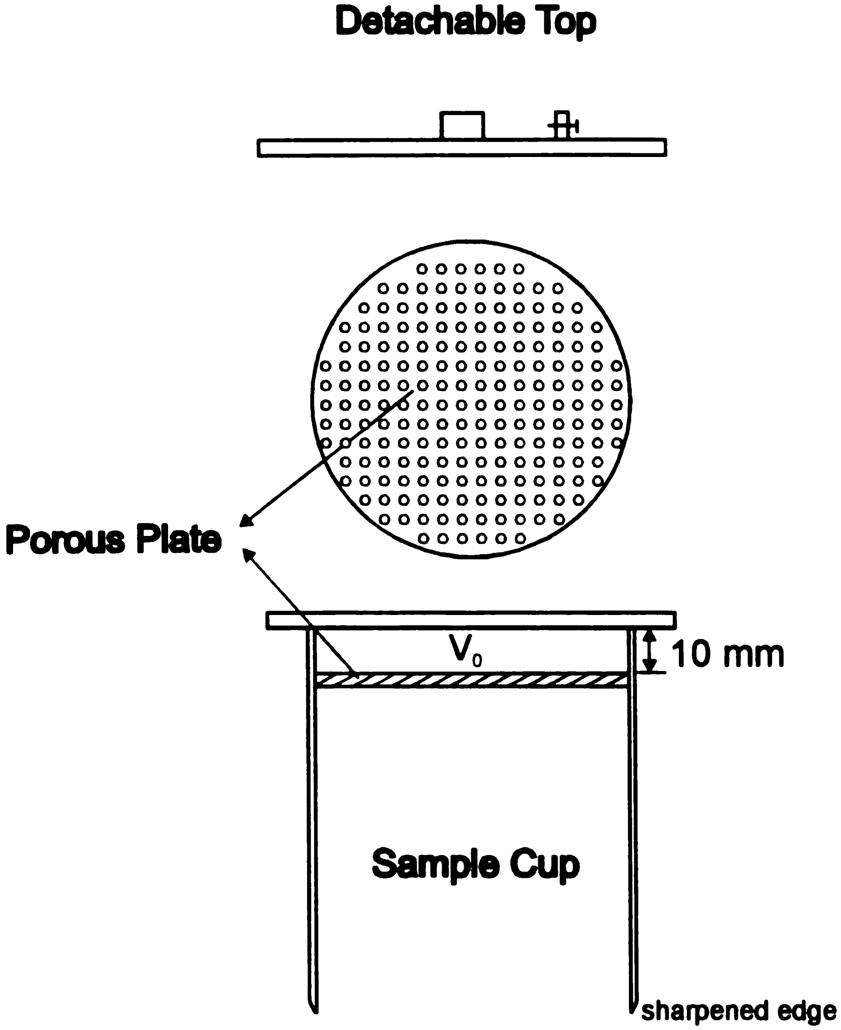
Detachable Top
Porous Plate
V_0
10 mm
Sample Cup
sharpened edge

Figure 29. Recommended sample cup and porous plate.

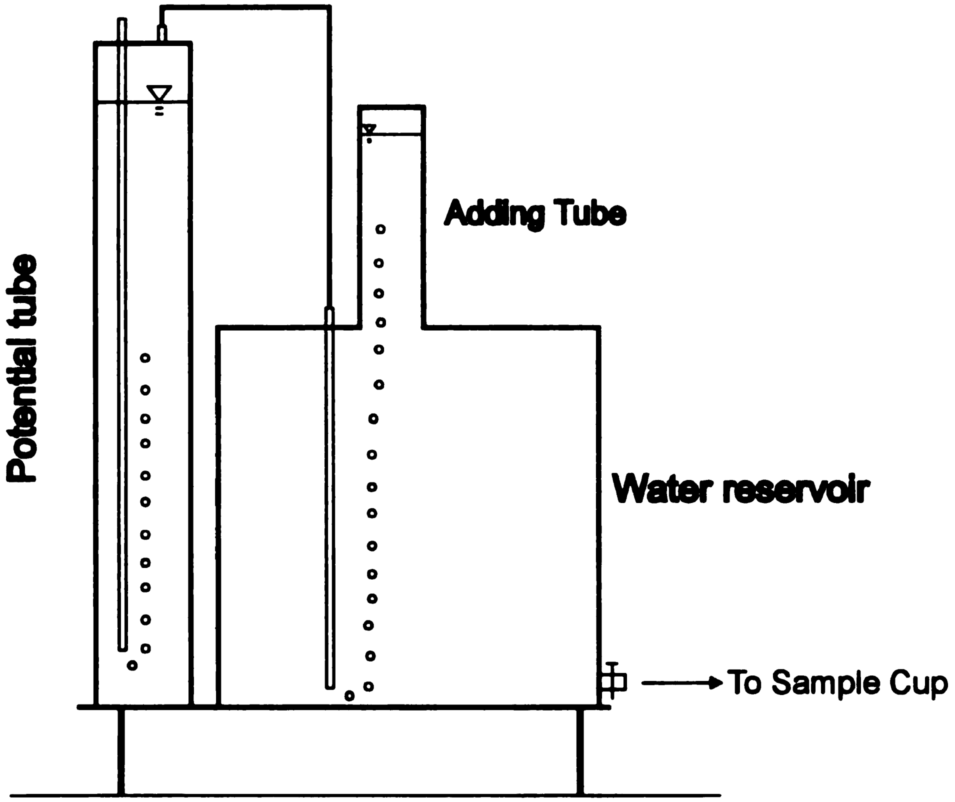
Potential tube
Adding Tube
Water reservoir
To Sample Cup

Figure 30. Recommended water reservoir with adding tube.

disk permeameter, and iii) the system has lower gravity center than disk permeameter to avoid wind effect and decline in the field.

The other problem was the reduction of the initial infiltration. Since the lag time t_0 is changing with the I_0, if the I_0 can be reduced, the t_0 will also decrease. This can ensure that the sorptivity flow still happen at the beginning of the measurement. In the prototype, the interconnecting tubing between the water reservoir and the sample cup was 3.2 mm inside diameter. Since the small tubing restricted the flow rate of filling water, this created more time and water to fill up the sample cup . A double tubing design (Fig. 31) is recommended to solve this problem. A 0.95 mm I. D. tubing is placed parallel to the flow meter and connected by two Y adapters. The parallel tubing will carry most water to the sample cup during the water filling. Once the sample cup is filled, shut the stopcock, and then the water will flow only through the flow meter. This device can reduce the I_0 and t_0 effectively and will increase the accuracy of the sorptivity measurement. The recommended range of t_0 for each soil is shown in Table 7 and decided by field experiences. If the calculated t_0 is over this range, the sorptivity would probably cease before the measurement starts.

Table 7. The recommended range of lag time for different soils.

TYPE OF SOIL	RANGE OF T0
Sand	$t_0 < 3$ minutes
Loam	$t_0 < 7$ minutes
Clay	$t_0 < 20$ minutes

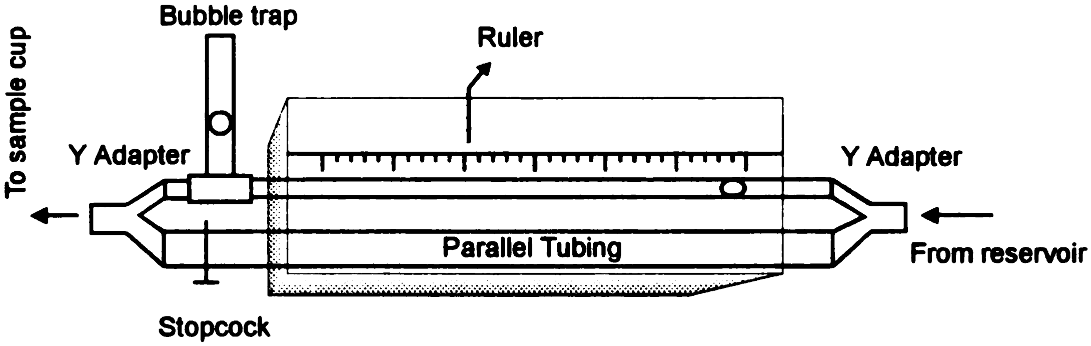
Bubble trap
Ruler
To sample cup
Y Adapter
Y Adapter
Parallel Tubing
From reservoir
Stopcock

Figure 31. Recommended flow meter with parallel tubing.

XI. Conclusions

The designed permeameter is an non-electronic system to measure the soil sorptivity in the field. It is low-cost, portable, reliable, and simple for installation and use. The infiltrometer can execute a test without air infiltration into the soil during conduct of the test, and can ensure the flow in one dimension during the early infiltration. Moreover, it has a large water capacity sufficient for a long term experiment and is satisfactory for sand, silt, loam, or clay textured soils. Moreover, the infiltrometer enables tests to be run under -10 mm to -150 mm water potential, and can measure a flow ranging 1 ml/min to 20 ml/min with tolerable error. In additional to the soil sorptivity, this instrument can be used to determine other hydraulic properties, (e.g. hydraulic conductivity, macroscopic capillary length, etc.) even in clay textured soils.

In the past, the i vs. $t^{1/2}$ diagram was used to determine the sorptivity through the application of Philip's equation. However, the derived sorptivity included some errors form the data analysis. The method proposed in this text enables the analysis of the soil sorptivity from the field data. Instead of the conventional i vs. $t^{1/2}$ diagram, the sorptivity is determined from an i^2 vs. t diagram, even when the true infiltration is not measured at the very start.

Two new parameters, initial infiltration and lag time, were introduced in the determination of the sorptivity. The initial infiltration is the amount of water infiltrated into soil before the infiltrometer water potential reaches the desired value. The initial infiltration becomes the interception in the i^2 vs. t diagram and can be measured at the onset of infiltration by the designed infiltrometer. The lag time is the duration between the onset of infiltration and the start of the measurement. It can be derived from the initial infiltration and the derived sorptivity. The lag time should be used to examine the reliability of the result of each experiment, since If the lag time is greater than the duration of the sorptivity flow, the derived sorptivity can not represent the true characteristic of the tested soil. Both initial infiltration and lag time are important for the determination of the sorptivity.

APPENDICES

APPENDIX A

APPENDIX A

COMPONENT SPECIFICATIONS

(All information given is from manufacture's system user's guide)

Digital Scale (K Tron DS-1)

- Size
  330 mm W X 124 mm H X 225 mm D.
- Capacity
  30 kg (66 lb).
- Readability
  0-6.0 kg (15 lb): 0.001 kg (0.003 lb).
  6.0-15 kg (30 lb): 0.005 kg (0.01 lb).
  15-30 kg (66 lb): 0.010 kg (0.02 lb).
- RS232 communications
  An RS232 port, accessible from a program, to communicate with the data logger.
- Battery capacity
  12 VDC, 1.4 AH.

Digital Scale (Denver Instrument, XL-500)

- Pan Size
  140 mm X 140 mm.
- Capacity
  500 g.
- Readability
  0.01 g.
- Response Time (avg.)
  3 sec.
- RS232 communications
  An RS232 port, accessible from a program, to communicate with the data logger.

Computer (Panasonic CF-150B)

- Size and weight
  309 mm W X 62 mm H X 250 mm D.
  2.9 kg (6.4 lb).

* CPU
  V20, 8 MHz.
* Memory
  640 K bytes.
* Storage
  3 1/2" Floppy Disk Driver.
  (720 K bytes double-sided, double density)
* Software
  MS-DOS 3.30, GW-BASIC 3.2.
* Battery capacity
  6 VDC, 1.8 AH.

APPENDIX B

APPENDIX B

Experimental Data for Field Tests

Experimental data for Test 2

t (sec)	t^2	Q (ml)	I (ml)	i (mm)	i^2
0	0.00	42.00	42.00	4.99	24.92
30	5.48	4.73	46.73	5.55	30.86
60	7.75	4.68	51.41	6.11	37.35
90	9.49	4.60	56.02	6.66	44.33
120	10.95	4.19	60.20	7.16	51.21
150	12.25	4.39	64.59	7.68	58.94
180	13.42	4.13	68.72	8.17	66.71
210	14.49	4.34	73.05	8.68	75.40
240	15.49	4.43	77.49	9.21	84.83
270	16.43	4.17	81.65	9.71	94.20
300	17.32	4.09	85.74	10.19	103.87
330	18.17	4.13	89.87	10.68	114.11
360	18.97	3.32	93.19	11.08	122.70
390	19.75	4.09	97.28	11.56	133.70
420	20.49	2.95	100.23	11.91	141.94
450	21.21	3.86	104.09	12.37	153.08
480	21.91	3.77	107.87	12.82	164.39
510	22.58	3.61	111.48	13.25	175.57
540	23.24	3.58	115.06	13.68	187.04
570	23.87	3.52	118.58	14.09	198.66
600	24.49	3.15	121.73	14.47	209.35
660	25.69	6.98	128.71	15.30	234.06
720	26.83	6.07	134.78	16.02	256.66
780	27.93	6.98	141.77	16.85	283.95
840	28.98	6.87	148.64	17.67	312.13
900	30.00	6.98	155.62	18.50	342.15
960	30.98	6.93	162.54	19.32	373.29
1020	31.94	7.01	169.56	20.15	406.20
1080	32.86	7.01	176.57	20.99	440.47
1140	33.76	7.13	183.70	21.84	476.78
1200	34.64	6.98	190.68	22.67	513.72

1260	35.50	7.10	197.79	23.51	552.70
1320	36.33	7.22	205.00	24.37	593.78
1380	37.15	7.22	212.22	25.23	636.33
1440	37.95	7.07	219.30	26.07	679.46

Experimental data for the first test at site 1

t (min)	Q (ml)	I (ml)	i (mm)	i^2
0	11.000	11.000	1.308	1.710
1	0.455	11.455	1.362	1.854
2	0.455	11.910	1.416	2.004
3	0.422	12.332	1.466	2.149
4	0.377	12.708	1.511	2.282
5	0.373	13.081	1.555	2.417
6	0.373	13.454	1.599	2.557
7	0.370	13.824	1.643	2.700
8	0.367	14.191	1.687	2.845
9	0.366	14.556	1.730	2.994
10	0.385	14.942	1.776	3.154
12	0.776	15.718	1.868	3.490
14	0.770	16.488	1.960	3.841
16	0.776	17.263	2.052	4.211
18	0.775	18.038	2.144	4.597
20	0.731	18.770	2.231	4.977
22	0.771	19.541	2.323	5.395
24	0.770	20.311	2.414	5.829
26	0.776	21.087	2.506	6.282
28	0.760	21.847	2.597	6.743
30	0.770	22.617	2.688	7.227
33	1.077	23.694	2.816	7.932
36	1.171	24.865	2.956	8.735
39	1.195	26.060	3.098	9.595
42	1.051	27.110	3.222	10.384
45	1.085	28.195	3.351	11.232
48	1.104	29.299	3.483	12.128
51	1.080	30.379	3.611	13.039
54	1.095	31.474	3.741	13.996
57	1.055	32.528	3.866	14.949
60	1.085	33.613	3.995	15.963
63	1.052	34.665	4.120	16.978
66	1.095	35.760	4.251	18.068

69	1.054	36.814	4.376	19.148
72	1.074	37.888	4.504	20.282
75	1.081	38.969	4.632	21.456
78	1.093	40.063	4.762	22.677
81	1.072	41.134	4.889	23.906
84	1.084	42.218	5.018	25.182
87	1.097	43.315	5.149	26.507
90	1.088	44.402	5.278	27.856

Experimental data for the second test at site 1

t (min)	Q (ml)	I (ml)	i (mm)	i^2
0	10.000	10.000	1.189	1.413
1	0.456	10.456	1.243	1.545
2	0.419	10.875	1.293	1.671
3	0.402	11.277	1.340	1.797
4	0.390	11.667	1.387	1.923
6	0.748	12.415	1.476	2.178
8	0.700	13.116	1.559	2.430
10	0.642	13.758	1.635	2.674
12	0.631	14.389	1.710	2.925
14	0.624	15.012	1.784	3.184
16	0.610	15.622	1.857	3.448
18	0.557	16.179	1.923	3.698
20	0.575	16.754	1.991	3.966
22	0.565	17.319	2.059	4.238
24	0.556	17.875	2.125	4.514
26	0.559	18.434	2.191	4.801
28	0.530	18.964	2.254	5.081
30	0.528	19.492	2.317	5.368
32	0.526	20.018	2.379	5.661
34	0.508	20.526	2.440	5.953
36	0.520	21.046	2.502	6.258
38	0.511	21.557	2.562	6.566
40	0.480	22.037	2.619	6.861
42	0.466	22.502	2.675	7.154
44	0.443	22.945	2.727	7.438
47	0.708	23.652	2.811	7.904
50	0.708	24.360	2.895	8.384
52	0.541	24.900	2.960	8.760
55	0.712	25.613	3.044	9.269

59	0.832	26.445	3.143	9.880
61	0.467	26.912	3.199	10.232
63	0.480	27.392	3.256	10.601
65	0.491	27.883	3.314	10.984
67	0.472	28.354	3.370	11.359
69	0.525	28.879	3.433	11.784
71	0.507	29.386	3.493	12.201
73	0.501	29.887	3.552	12.620
75	0.525	30.412	3.615	13.067
77	0.501	30.913	3.674	13.501
79	0.531	31.444	3.737	13.969
81	0.455	31.899	3.792	14.376

Experimental data for the first test at site 2

t (sec)	Q (ml)	I (ml)	i (mm)	i^2
0	27.000	27.000	3.209	10.300
60	4.190	31.190	3.707	13.744
120	4.110	35.299	4.196	17.605
180	4.104	39.403	4.684	21.936
240	4.004	43.407	5.159	26.620
300	3.805	47.212	5.612	31.492
360	3.789	51.001	6.062	36.750
420	3.763	54.764	6.509	42.373
480	3.719	58.483	6.951	48.323
540	3.510	61.993	7.369	54.299
600	3.452	65.445	7.779	60.513
660	3.342	68.787	8.176	66.851
720	3.325	72.112	8.572	73.471
780	3.325	75.438	8.967	80.404
840	3.309	78.747	9.360	87.613
900	3.291	82.038	9.751	95.088
960	3.239	85.277	10.136	102.745
1020	3.224	88.500	10.519	110.659
1080	3.149	91.649	10.894	118.674
1140	3.141	94.790	11.267	126.948
1200	2.907	97.698	11.613	134.855
1320	5.612	103.310	12.280	150.793
1440	5.384	108.694	12.920	166.921
1560	5.258	113.952	13.545	183.460
1680	5.230	119.182	14.166	200.687

1800	5.143	124.325	14.778	218.381
1920	5.194	129.519	15.395	237.011
2040	5.300	134.820	16.025	256.807
2160	5.143	139.962	16.636	276.771
2280	5.214	145.177	17.256	297.777
2400	5.195	150.372	17.874	319.471

Experimental data for the second test at site 2

t (sec)	Q (ml)	I (ml)	i (mm)	i^2
0	25.000	25.000	2.972	8.830
60	3.722	28.722	3.414	11.656
120	3.700	32.423	3.854	14.852
180	3.682	36.104	4.291	18.417
240	3.646	39.750	4.725	22.324
300	3.585	43.335	5.151	26.533
360	3.585	46.920	5.577	31.104
420	3.581	50.501	6.003	36.033
480	3.567	54.068	6.427	41.303
540	3.563	57.632	6.850	46.927
600	3.546	61.178	7.272	52.879
660	3.419	64.596	7.678	58.954
720	3.368	67.965	8.079	65.262
780	3.368	71.333	8.479	71.892
840	3.353	74.686	8.877	78.809
900	3.335	78.021	9.274	86.004
960	3.301	81.322	9.666	93.436
1020	3.287	84.610	10.057	101.143
1080	3.285	87.895	10.447	109.150
1140	3.239	91.133	10.832	117.342
1200	3.207	94.340	11.214	125.745
1320	6.182	100.523	11.948	142.766
1440	6.067	106.589	12.670	160.519
1560	5.912	112.502	13.372	178.820
1680	5.870	118.372	14.070	197.969
1800	5.687	124.059	14.746	217.449
1920	5.659	129.718	15.419	237.739
2040	5.545	135.264	16.078	258.500
2160	5.674	140.938	16.752	280.642
2280	6.020	146.957	17.468	305.127
2400	5.650	152.607	18.139	329.040

Experimental data for the third test at site 2

t (sec)	Q (ml)	I (ml)	i (mm)	i^2
0	24.000	24.000	2.853	8.138
60	3.904	27.904	3.317	11.001
120	3.520	31.425	3.735	13.952
180	3.371	34.795	4.136	17.106
240	3.174	37.969	4.513	20.368
300	3.142	41.111	4.887	23.879
360	3.058	44.170	5.250	27.564
420	3.058	47.228	5.614	31.514
480	3.051	50.279	5.976	35.716
540	3.013	53.292	6.334	40.125
600	3.013	56.305	6.693	44.791
660	2.930	59.235	7.041	49.574
720	2.923	62.158	7.388	54.587
780	2.922	65.080	7.736	59.841
840	2.916	67.996	8.082	65.323
900	2.903	70.899	8.427	71.020
960	2.896	73.795	8.771	76.939
1020	2.896	76.690	9.116	83.096
1080	2.882	79.573	9.458	89.459
1140	2.863	82.436	9.799	96.013
1200	2.863	85.299	10.139	102.798
1260	2.856	88.155	10.478	109.797
1320	2.836	90.991	10.816	116.975
1380	2.830	93.821	11.152	124.365
1440	2.824	96.645	11.488	131.965
1500	2.726	99.372	11.812	139.516
1560	2.824	102.196	12.147	147.559
1620	2.775	104.971	12.477	155.680
1680	2.780	107.751	12.808	164.036
1740	2.630	110.381	13.120	172.141
1800	2.698	113.078	13.441	180.657
1920	5.382	118.460	14.081	198.263
2040	5.149	123.609	14.693	215.874
2160	5.204	128.814	15.311	234.435
2280	5.429	134.243	15.957	254.612
2400	5.318	139.561	16.589	275.185

Experimental data for the first at site 3

t (sec)	Q (ml)	I (ml)	i (mm)	i^2
0	28.000	28.000	3.328	11.077
20	3.741	31.741	3.773	14.235
40	3.535	35.276	4.193	17.582
60	3.454	38.730	4.604	21.193
80	3.573	42.303	5.028	25.284
100	3.535	45.838	5.448	29.686
120	3.409	49.247	5.854	34.265
140	3.375	52.622	6.255	39.123
160	3.300	55.922	6.647	44.183
180	3.170	59.092	7.024	49.335
200	3.130	62.221	7.396	54.699
220	3.115	65.336	7.766	60.312
240	3.068	68.404	8.131	66.109
260	3.103	71.507	8.500	72.244
280	3.144	74.652	8.873	78.736
300	3.004	77.656	9.230	85.202
360	9.069	86.725	10.308	106.264
420	9.069	95.794	11.386	129.651
480	8.983	104.778	12.454	155.108
540	8.905	113.682	13.513	182.593
600	9.019	122.702	14.585	212.716
660	8.918	131.620	15.645	244.762
720	9.062	140.683	16.722	279.627
780	9.204	149.887	17.816	317.412
840	8.944	158.830	18.879	356.422
900	8.831	167.662	19.929	397.160
960	8.880	176.542	20.984	440.345
1020	8.705	185.247	22.019	484.843
1080	8.718	193.965	23.055	531.549
1140	8.983	202.948	24.123	581.926
1200	8.944	211.892	25.186	634.345
1260	9.025	220.916	26.259	689.530
1320	8.864	229.780	27.313	745.973
1380	8.849	238.629	28.364	804.538
1440	8.996	247.626	29.434	866.343
1500	8.913	256.539	30.493	929.833
1560	8.838	265.377	31.544	995.002

1620	8.819	274.196	32.592	1062.235
1680	9.037	283.233	33.666	1133.405
1740	8.887	292.119	34.722	1205.644
1800	8.913	301.033	35.782	1280.341

Experimental data for the second test at site 3

t (sec)	Q (ml)	I (ml)	i (mm)	i^2
0	30.000	30.000	3.566	12.716
20	3.541	33.541	3.987	15.895
40	3.528	37.069	4.406	19.414
60	3.441	40.511	4.815	23.186
80	3.320	43.830	5.210	27.142
100	3.398	47.229	5.614	31.514
120	3.086	50.314	5.981	35.767
140	3.136	53.450	6.353	40.364
160	3.048	56.498	6.716	45.099
180	3.046	59.544	7.078	50.092
200	2.988	62.531	7.433	55.245
220	2.915	65.446	7.779	60.515
240	3.068	68.514	8.144	66.322
260	2.949	71.463	8.494	72.155
280	3.004	74.468	8.852	78.349
300	3.004	77.472	9.209	84.799
360	8.909	86.381	10.268	105.424
420	8.744	95.125	11.307	127.847
480	9.033	104.158	12.381	153.280
540	9.033	113.192	13.454	181.020
600	8.849	122.041	14.506	210.430
660	8.804	130.845	15.553	241.888
720	8.983	139.829	16.621	276.242
780	9.217	149.046	17.716	313.861
840	8.870	157.916	18.770	352.330
900	8.962	166.878	19.836	393.456
960	8.907	175.785	20.895	436.580
1020	8.832	184.617	21.944	481.553
1080	8.373	192.991	22.940	526.226
1140	8.243	201.234	23.919	572.140
1200	8.455	209.690	24.924	621.230
1260	8.772	218.461	25.967	674.291
1320	8.438	226.900	26.970	727.387

1380	8.129	235.029	27.936	780.442
1440	8.125	243.154	28.902	835.334
1500	8.262	251.416	29.884	893.066
1560	8.554	259.969	30.901	954.867
1620	8.174	268.144	31.873	1015.859
1680	8.374	276.518	32.868	1080.299
1740	8.595	285.113	33.890	1148.504
1800	8.174	293.287	34.861	1215.303

Experimental data for the third test at site 3

t (sec)	Q (ml)	I (ml)	i (mm)	i^2
0	34.000	34.000	4.041	16.333
30	3.806	37.806	4.494	20.194
60	3.760	41.567	4.941	24.411
90	3.741	45.308	5.385	29.003
120	3.659	48.967	5.820	33.876
150	3.626	52.593	6.251	39.079
180	3.565	56.157	6.675	44.556
210	3.492	59.649	7.090	50.269
240	3.448	63.097	7.500	56.248
270	3.380	66.476	7.902	62.435
300	3.353	69.829	8.300	68.892
330	3.353	73.181	8.699	75.666
360	3.296	76.478	9.090	82.636
390	3.309	79.787	9.484	89.942
420	3.313	83.100	9.878	97.566
450	3.125	86.225	10.249	105.042
480	3.247	89.472	10.635	113.103
510	3.237	92.709	11.020	121.433
540	3.237	95.945	11.404	130.060
570	3.036	98.981	11.765	138.422
600	3.212	102.193	12.147	147.551
660	6.445	108.638	12.913	166.748
720	6.445	115.083	13.679	187.119
780	6.445	121.527	14.445	208.664
840	6.375	127.902	15.203	231.130
900	6.420	134.323	15.966	254.915
960	6.470	140.792	16.735	280.062
1020	6.445	147.237	17.501	306.288
1080	6.230	153.467	18.242	332.757

1140	6.498	159.965	19.014	361.532
1200	6.466	166.431	19.783	391.350
1260	6.470	172.900	20.552	422.367
1320	6.470	179.370	21.321	454.566
1380	6.470	185.839	22.090	487.948
1440	6.420	192.259	22.853	522.244
1500	6.593	198.852	23.636	558.674
1560	6.494	205.346	24.408	595.762
1620	6.473	211.820	25.178	633.914
1680	6.396	218.215	25.938	672.773
1740	6.494	224.710	26.710	713.415
1800	6.523	231.233	27.485	755.436

Experiment data for initial water content and final water content of each replication at site 3

B.K. = 1470 kg / m^3

	W_1 (g)	W_2 (g)	W_3 (g)	W.C. (%)	Volumetric W.C (%)
Test 1	21.8	139.78	120.22	19.874	29.215
Test 2	22.44	119.65	103.63	19.731	29.005
Test 3	21.93	133.59	115.37	19.499	28.664
Before	22.1	140.11	136.3	3.336	4.904

Where

W_1: weight of tin can

W_2: weight of tin can and wet soil

W_3: weight of tin can and dry soil

APPENDIX C

APPENDIX C

Experimental Data for Error Analysis

V_b (cm/sec)	Q (ml/min)	log V_b	log Q	Q_{before}	Q_{after}	Err_{before}^2	Err_{after}^2
0.894	4.189	-0.048	0.622	4.188	4.249	2E-06	0.0036
1.054	4.932	0.023	0.693	4.881	5.007	0.0026	0.0057
0.972	4.532	-0.012	0.656	4.525	4.617	6E-05	0.0071
1.119	5.152	0.049	0.712	5.161	5.316	7E-05	0.0266
1.249	5.704	0.097	0.756	5.720	5.936	0.0003	0.0534
1.167	5.356	0.067	0.729	5.369	5.545	0.0002	0.036
1.280	5.796	0.107	0.763	5.850	6.080	0.0029	0.0805
1.393	6.331	0.144	0.801	6.333	6.619	3E-06	0.0829
1.501	6.752	0.176	0.829	6.787	7.129	0.0013	0.1425
1.411	6.415	0.150	0.807	6.408	6.703	5E-05	0.0832
1.319	6.002	0.120	0.778	6.018	6.267	0.0003	0.0702
1.386	6.310	0.142	0.800	6.303	6.586	5E-05	0.0758
1.514	6.856	0.180	0.836	6.841	7.190	0.0002	0.1119
1.612	7.333	0.207	0.865	7.256	7.658	0.0061	0.1052
1.930	8.583	0.285	0.934	8.581	9.167	2E-06	0.3408
2.408	10.555	0.382	1.023	10.553	11.441	4E-06	0.7851
2.945	12.735	0.469	1.105	12.733	13.991	8E-06	1.5773
3.211	13.803	0.507	1.140	13.800	15.252	1E-05	2.0991
				Sum square error:		0.001	0.3159

V_b : velocity of bubble.

Q : discharge of real flow.

$Q_{berfore}$: predicted flow rate by velocity of bubble.

Q_{after} : predicted flow rate by Eq. (10).

Err_{before} : error between $Q_{berfore}$ and Q.

Err_{after} : error between Q_{after} and Q.

LIST OF REFERENCES

LIST OF REFERENCES

Ankeny, M. D. , T. C. Kaspar, and R. Horton. 1988. Design for an automated tension infiltrometer. Soil Sci. Sco. Am. J. 52:893-896.

Bridge, B.J., and P. J. Ross. 1985. A portable microcomputer-controlled drip infiltrometer. I . design and operation. Aust. J. Soil Res. 23:383-391.

Clothier, B. E., and I. White. 1981. Measurement of sorptivity and soil water diffusivity in the field. Soil Sci. Sco. Am. J. 45:241-245.

Dirksen, C. 1975. Determination of soil water diffusivity by sorptivity measurement. Soil Sci. Sco. Am. Proc. 39:22-27.

Dixon, R. M. 1975. Design and use of closed-top infiltrometers. Soil Sci. Sco. Am. Proc. 39:755-763.

Logsdon, S. D., and D. B. Jaynes. 1993. Methodology for determining hydraulic conductivity with tension infiltrometer. Soil Sci. Sco. Am. J. 57: 1426-1431.

Perroux, K. M., and I. White. 1988. Design for disk permeameters. Soil Sci. Sco. Am. J. 52:1205-1215.

Philip, J. R. 1969. Theory of infiltration. Adv. Hydrosci. 5:215-296.

Reynolds W. D., and D. E. Eleric. 1985. In situ measurement of field-saturated hydraulic conductivity, sorptivity, and the alpha-parameter using the Guelph permeameter. Soil Sci.140:292-302.

Scotter, D. R., B. E. Clothier, and E. R. Harper. 1982. Measuring saturated hydraulic conductivity and sorptivity using twin rings. Aust. J. Soil Res. 20:295-304.

Talsma, T. 1969. In situ measurement of sorptivity. Aust. J. Soil Res. 7:269-276.

White, I., and M. J. Sully. 1987. Macroscopic and microscopic capillary length and time scales from field infiltration. Water Resour. Res. 23: 1514-1522.

Wooding, R. A. 1968. Steady infiltration from a shallow circular pond. Water Resour. Res. 4:1259-1273.

MICHIGAN STATE UNIV. LIBRARIES
31293017129101